AD NUMBER

AD212400

LIMITATION CHANGES

TO:

Approved for public release; distribution is unlimited.

FROM:

**Distribution authorized to U.S. Gov't. agencies and their contractors;
Administrative/Operational Use; OCT 1957. Other requests shall be referred to Office of Naval Research, 875 N. Randolph St., Arlington, VA 22203.**

AUTHORITY

ONR ltr, 15 Jun 1977

UNIVERSITY OF CALIFORNIA SCRIPPS INSTITUTION OF OCEANOGRAPHY

REPRINT

WAVE-GENERATED RIPPLES IN NEARSHORE SANDS

By Douglas L. Inman

From Beach Erosion Board,
Department of the Army,
Corps of Engineers,
Technical Memorandum No. 100
October, 1957

This paper represents results of research carried out by the University of California under Contract DA-49-eng-3 with the Beach Erosion Board and Contract Nonr-2216(01) with the Office of Naval Research.

1 February 1958

WAVE-GENERATED RIPPLES IN NEARSHORE SANDS

DEPARTMENT OF THE ARMY
CORPS OF ENGINEERS
TECHNICAL MEMORANDUM NO.100

OCTOBER 1957

FOREWORD

A study of the occurrence of sand ripples generated by wave action in the nearshore area has been made based on observations of swimmers equipped with self-contained underwater breathing apparatus. Such parameters as the symmetry of the ripples, and their wave length and crest length, were measured and are related to the sand size, and to the orbital velocity and displacement of the wave motion generating the ripples. It was felt that publication of this data would be of interest to workers in the coastal engineering and geology fields as presenting additional data to aid in the understanding of nearshore processes and the factors influencing longshore movement of material, in particular the mechanisms of ripple formation and growth. This report presents the results of this study.

In general the ripple size increased with an increase in sand size and, to a certain extent, with water depth. Ripples in more exposed areas were generally larger than those in sheltered bays. Ripples were always present when the orbital velocity was between about 0.3 and 3 feet per second.

This report was prepared at the Scripps Institution of Oceanography of the University of California in pursuance of contracts with the Beach Erosion Board and the Office of Naval Research. The author of the report, D. L. Inman, is a member of the staff of Scripps Institution of Oceanography.

Views and Conclusions expressed in this report are not necessarily those of the Beach Erosion Board or the Office of Naval Research.

This report is published under authority of Public Law 166, 79th Congress, approved July 31, 1945.

TABLE OF CONTENTS

WAVE-GENERATED RIPPLES IN NEARSHORE SANDS*

by
Douglas L. Inman
University of California
Scripps Institution of Oceanography
La Jolla, California

ABSTRACT

A study of the formation and occurrence of sand ripples generated by oscillatory wave motion was made in coastal waters to gain a better understanding of the role ripples play in the sorting and transportation of sediments. The observations, which extend from the surf zone to depths of about 170 feet, were made by swimmers equipped with self-contained underwater breathing apparatus. The wave length, crest length, height and symmetry of the ripples were measured and these parameters compared with the size of the sand and with the orbital displacement and velocity of the wave motion generating the ripples.

Ripples were always present on sandy bottoms when the significant orbital velocity had a value between about 1/3 and 3 feet per second. The type of ripple was related to the size of the sand and the nature and rigor of wave motion. The ripple wave length ranged from 0.14 feet in fine sand to over 4 feet in very coarse sands. The heights of the ripples ranged from about one-fourth to one-sixteenth of the ripple wave length.

In areas of abundant sand, the largest and least dense material occurred on the ripple crests and the finest and heaviest in the trough. Over rocky bottoms where there was little sand, the relationship was frequently reversed. The ripple crest consisted of sand washed from among the rocks, while the coarse material remained in the trough.

INTRODUCTION

Ripples are generally subdivided into current ripples and oscillatory ripples, depending on whether the motion leading to their formation was that of a unidirectional current as in streams and eolian transport or an oscillatory current as in wave motion. This paper treats the oscillatory type of sand ripples, which are defined here as the systematic series of undulations or waves that form at the sand-water interface under the influence of surface gravity waves. Such ripples form

*Contribution from the Scripps Institution of Oceanography, New Series No. 947

when the fluid stress on the bottom is slightly in excess of that required to initiate movement of sediment particles, and disappear when there is general bed motion at somewhat higher fluid velocities.

There is extensive literature on ripple marks; earlier work is listed in a bibliography on the subject by Kindle and Edwards (1924), and more recent work is summarized in papers by van Straaten (1953) and Manohar (1955). However, most investigations and measurements of ripple characteristics have been restricted to ancient rocks or small scale laboratory studies, or to ripple impressions exposed at low water or observed from the surface in quiet water. The advent of self-contained underwater breathing apparatus, which allows swimmers to move about freely and to make measurements and observations under water, has provided the means for measuring and studying ripples in motion and under natural circumstances (figure 1). The purpose of this paper is to describe oscillatory ripples as they occur in nature, especially in oceanic coastal waters, and to discuss their occurrence and physical characteristics in relation to the waves generating them.

METHOD

Most ripple observations and measurements in the present study were made along the sandy shelf bordering the coast of southern California, although the field work included observations from the narrow shelf fringing the Hawaiian Islands and the shelves of other islands along the coast of Mexico and California. In addition to coasts exposed to the open ocean, observations were made in other environments including protected coasts, bays, bays behind barrier reefs, and one observation from a model wave tank. In all, about 1,000 ripples were measured during almost 200 observations which were made in waters ranging in depth from a fraction of a foot to 170 feet. The ripples measured had wave lengths from 0.14 to over 4 feet. Whenever possible, as in 102 cases, surface waves were recorded during the period of ripple observation.

In addition to a wide geographic distribution of observations, ripples from specific areas were studied over long periods of time and under various wave conditions. A series of four stations ranging in depth from 18 to 70 feet below mean lower low water were visited frequently during a period of several years. These stations are located on D range, which is on the shelf off La Jolla, California, where the sediments consist of a relatively uniform, fine quartz sand (figure 2). In addition, four areas were visited frequently on the shelf off Point La Jolla at depths of 30, 40, 55, and 85 feet. The sediments at these areas differ markedly from those on D range in that they occur in large patches separated by low rock outcrops. Sediments are coarser, somewhat more rounded, have more shell fragments, and in general do not grade from one type to another. The stations on D range were established in conjunction with a study of the changes in level of the sandy bottom.

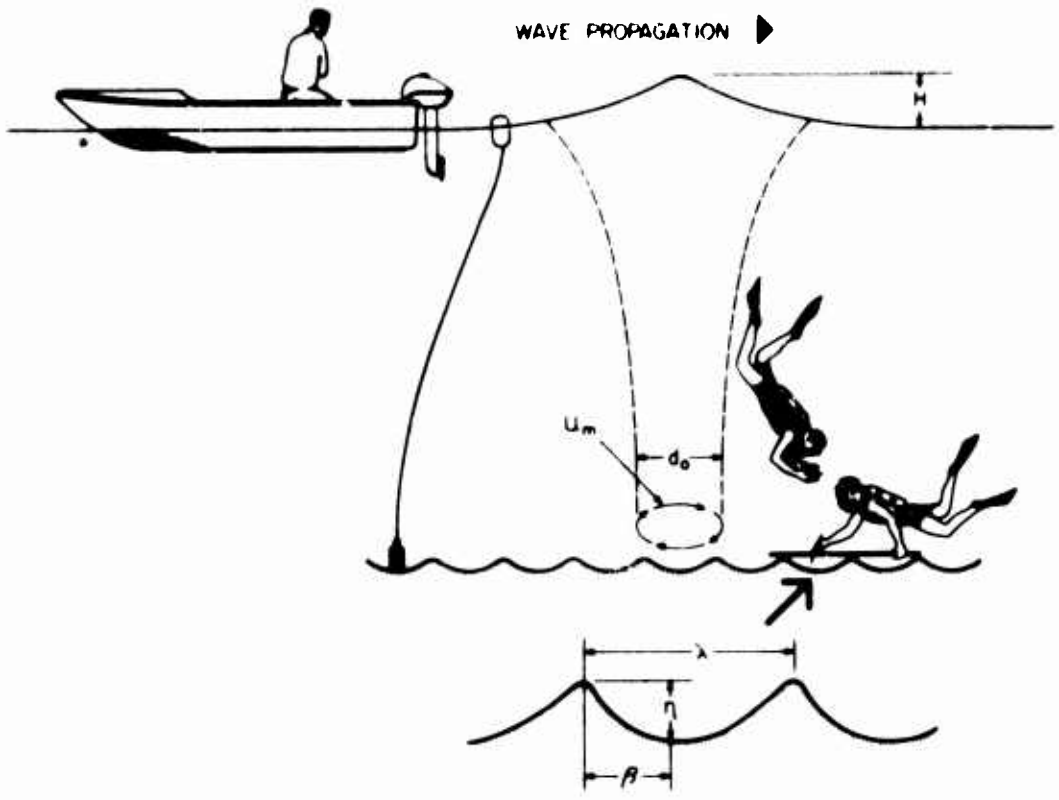

FIGURE 1 SCHEMATIC DIAGRAM ILLUSTRATING THE TECHNIQUE USED IN MEASURING RIPPLES AND THE NOTATION FOR DESCRIBING WAVES AND RIPPLES. (U_m is the maximum horizontal orbital velocity of the waves, and d_o is the orbital diameter near the bottom. λ is the ripple wave length, η the ripple height, and λ/η and β/λ are the ripple index and measure of symmetry respectively.)

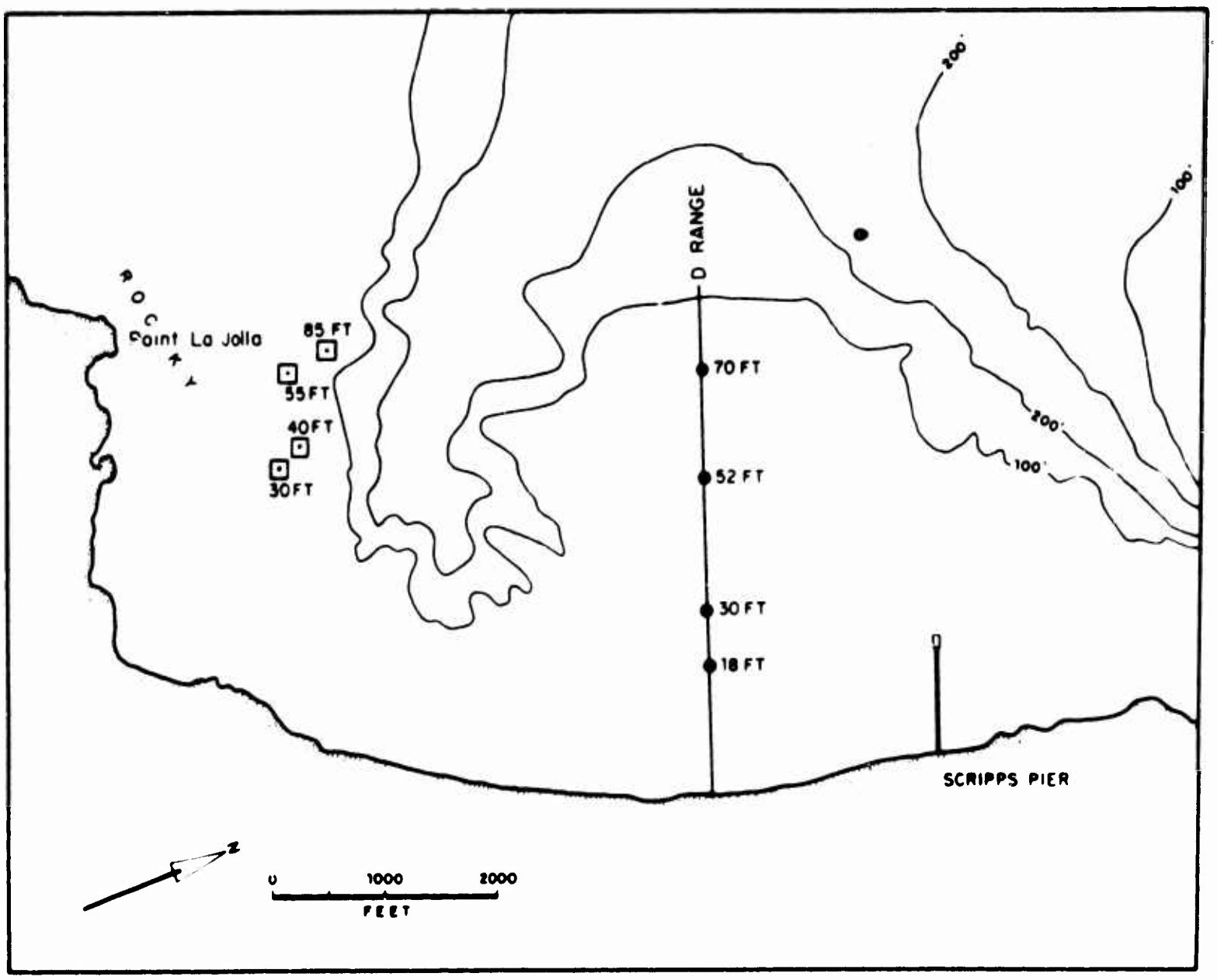

FIGURE 2 INDEX CHART SHOWING LOCATION AND DEPTH OF STATIONS ON THE SHELF OFF LA JOLLA, CALIFORNIA. Observations from the four stations on D range are tabulated chronologically in Appendix I A-I D, and those from the stations off Point La Jolla, California are listed by depth in Appendix II A

The changes in level between each ripple observation on this range are given by Inman and Rusnak (1956), and the description of the sediment characteristics and the hydrography of both areas is given by Inman (1953).

The collocation of all data was based primarily on the wave exposure of the area: observations from coasts exposed to the open ocean are tabulated in Appendices I and II; those from lee and protected coasts in Appendix III; and those from areas of limited fetch in Appendix IV. The most complete and systematic observations were made at the four stations on D range off La Jolla, and these are listed chronologivally by station in Appendix I. Observations from the four areas off Point La Jolla are listed under the appropriate depth in Appendix II-A.

Ripple Measurement

Various techniques were used in the measurement of ripples. The most convenient technique for smaller ripples was to mark the ripple dimensions on a transparent plastic strip which was placed on the bottom perpendicular to the ripple crests. The position of each ripple crest and trough and the height of the ripple were marked on the plastic with a grease pencil. After the diver returned to the surface, the markings on the plastic strip were measured and recorded. Three measures were obtained for each ripple: the wave length λ, which is the spacing between ripple crests; the ripple height η, which is the vertical distance from crest to trough; and the horizontal distance β, measured from the ripple crest to the deepest portion of the trough in the direction of propagation of the surface waves. These measurements are defined schematically in figure 1. λ and β for the smaller ripples were measured to the nearest hundredth of a foot and η to the nearest five thousandth of a foot. Since the positions of the ripple crests were usually quite sharp, λ is a reasonably accurate measure, while β, which depends on the lowest position of the concave ripple trough, is somewhat less accurate. η is the least accurate because it is the most difficult to measure and in fine sand the weight of the plastic strip tends to flatten the ripple crests.

The ratio of β to the wave length λ was used as a measure of ripple symmetry. Symmetrical ripples, insofar as the position of ripple crest and trough are concerned, have a value of β/λ equal to $\frac{1}{2}$. Values less or greater than $\frac{1}{2}$ indicate that the ripple has a tendency to be asymmetrical like a current ripple. If the ratio is less than $\frac{1}{2}$, the steep lee face of the ripple, faces in the direction of wave propagation, and if the value is greater than $\frac{1}{2}$ the opposite is true.

The ratio of ripple wave length to ripple height, λ/η, referred to as the "ripple index", is used in this study as a measure of ripple steepness. It is the inverse of the steepness measure commonly employed for wave phenomena.

The average values of ripple wave length λ , height η , and of the ratio λ/η and β/λ for each observation, together with the number of ripples measured are entered in the appendices. In cases where the data was inadequate to obtain numerical values of β, a notation was entered from the divers' observations indicating whether the ripples appear to be symmetrical, or if asymmetrical, whether they resembled current ripples resulting from onshore ($\beta/\lambda < \frac{1}{2}$) or offshore ($\beta/\lambda > \frac{1}{2}$) currents. In addition, if the ripple symmetry was observed to change with the passage of each wave crest and trough, the symmetry was recorded as "reversing".

A simple device was fabricated for more detailed measurement of the profile of large ripples. The device consisted of a series of parallel brass prongs welded at right angles to a metal bar so that the instrument has the appearance of a large comb (figure 3). The prongs were coated with grease so that when forced into the sand bottom, the imprint of the ripple profile was clearly marked in the grease. A spirit level was attached to the bar to permit the device to be leveled and thus give a profile of the ripple relative to a level datum. Representative profiles are shown in figure 4.

It became apparent during the study that ripple profiles could be broadly divided into two types: those with flat troughs separating the crests which, because of their resemblance to the analogous wave type were termed "solitary", and those with rounded troughs which were termed "trochoidal" (figures 5 and 6). In many cases, particularly for smaller ripples, it was not possible to measure the profiles accurately and the classification of solitary or trochoidal was determined from the visual observations of the diver. A "sawtooth" profile which is common in current ripples, was rarely observed in the oscillatory ripples.

Ripples were also classified as to pattern or plan, the basis of classification being the ratio of the average ripple crest length to wave length of the ripples. Long-crested ripples, that is, ripples with average crest lengths greater than 8 ripple wave lengths, were designated as pattern 1. Intermediate crested ripples, crest lengths between 3 and 8 λ , were designated as pattern 2, and short-crested ripples with crest lengths less than 3 λ as pattern 3 (see figures 6, 7 and 8). The limiting values of 3 and 8 λ were found to be most useful in dividing the ripples into three relatively discrete classes.

Whenever the water was clear, the ripples were photographed so that more leisurely study could be made in the laboratory. In this way the use of still photography accelerated the program by eliminating many of the intricacies of underwater observations and measurements. In addition, the mechanics of ripple movement, such as the change in ripple shape with time and the nature of the vortex formed in the ripple lee by each reversal in water motion were recorded and studied by motion pictures. Underwater motion pictures were made of ripples ranging in wave length from 0.2 to 3 feet.

FIGURE 3 DEVICE USED FOR MEASURING RIPPLE PROFILE. (The prongs were coated with grease so that when forced into the sand bottom the imprint of the ripple profile is clearly marked in the grease. A spirit level (not shown) was attached to the bar to give a level datum. Typical profiles are shown in figure 4)

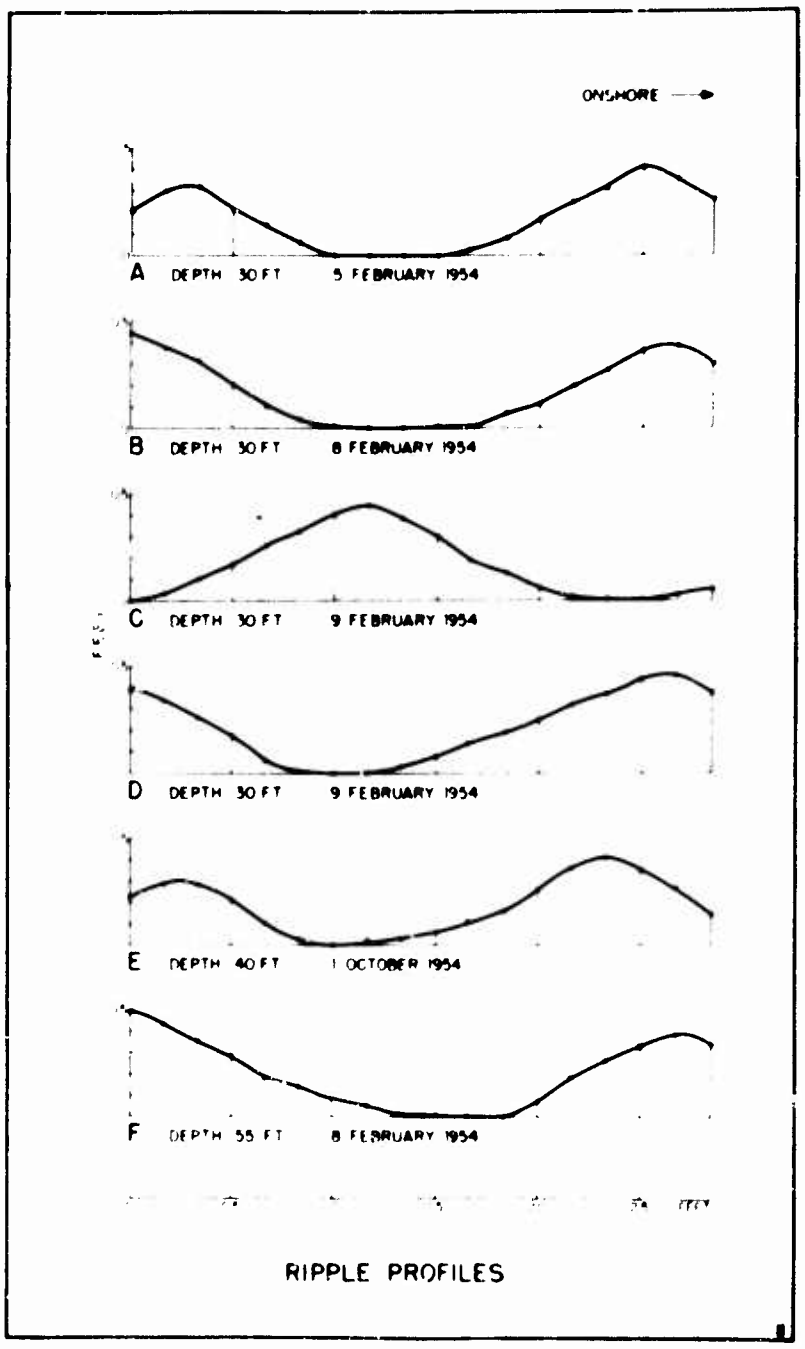

FIGURE 4. REPRESENTATIVE PROFILES OF LARGE RIPPLES FROM THREE STATIONS OFF POINT LA JOLLA, CALIFORNIA. Locations are shown by depths in figure 2, and complete descriptions are tabulated by depth and date in Appendix IIA.

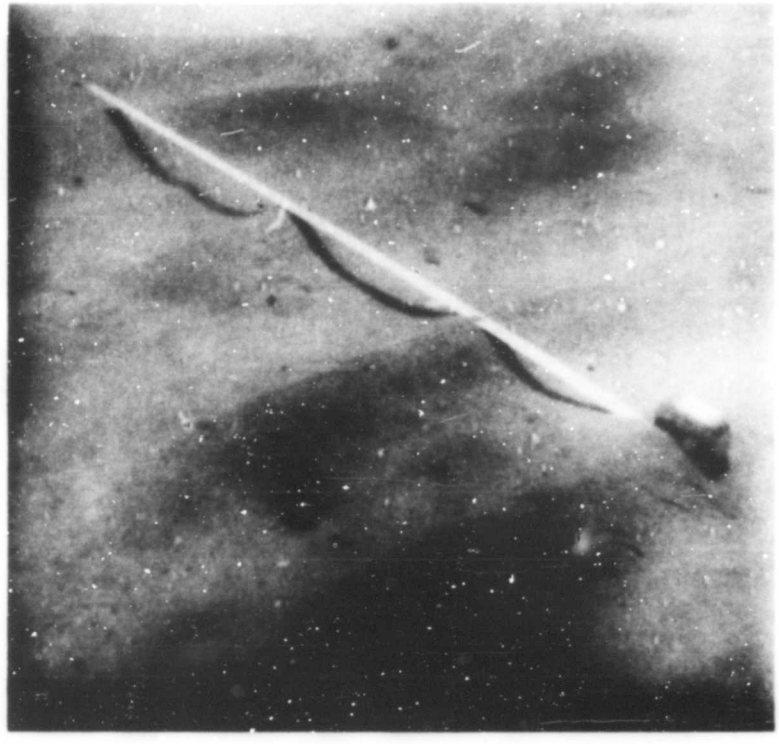

FIGURE 5. TROCHOIDAL RIPPLE PROFILE FROM THE PROTECTED SHELF OFF SAN CLEMENTE ISLAND, CALIFORNIA. Ripple wave length 0.67 ft., depth of water 21 ft. Sand on the ripple crest is slightly coarser than that in the trough. Complete description tabulated in Appendix III B

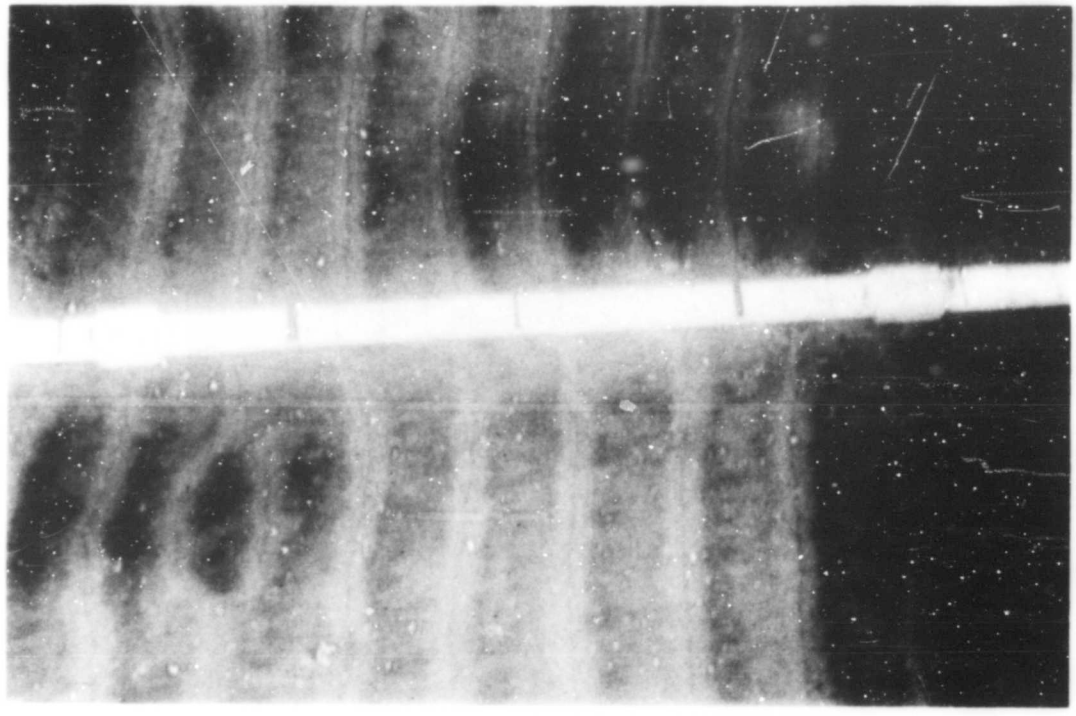

FIGURE 6. LONG-CRESTED RIPPLES (PATTERN 1) Ripples in fine sand at depth of 14 ft. on D range (Appendix I A, 2 August 1954). Ripple profile is "solitary" consisting of flat troughs separated by relatively sharp crests. Dark colored heavy minerals occur in the trough, light colored quartz sand in the crests, with a narrow line of dark mica at the apex of the crest. Each scale division is 0.1 ft.

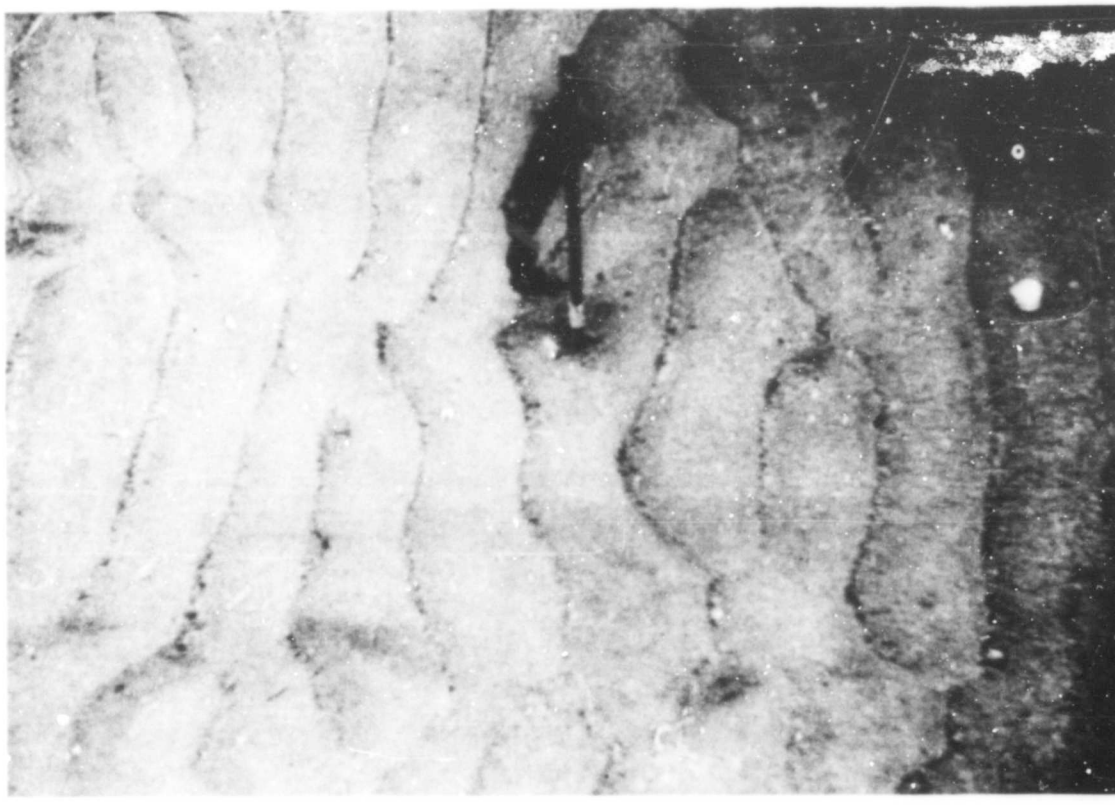

FIGURE 7. RIPPLES WITH INTERMEDIATE CREST LENGTHS (PATTERN 2). Ripples in fine sand at a depth of 30 ft on D range (Appendix I B, 21 August 1953). Ripple profile is solitary and the average wave length is 0.22 ft. Reference rod is used for measuring changes in sand level (Inman and Rusnak, 1956).

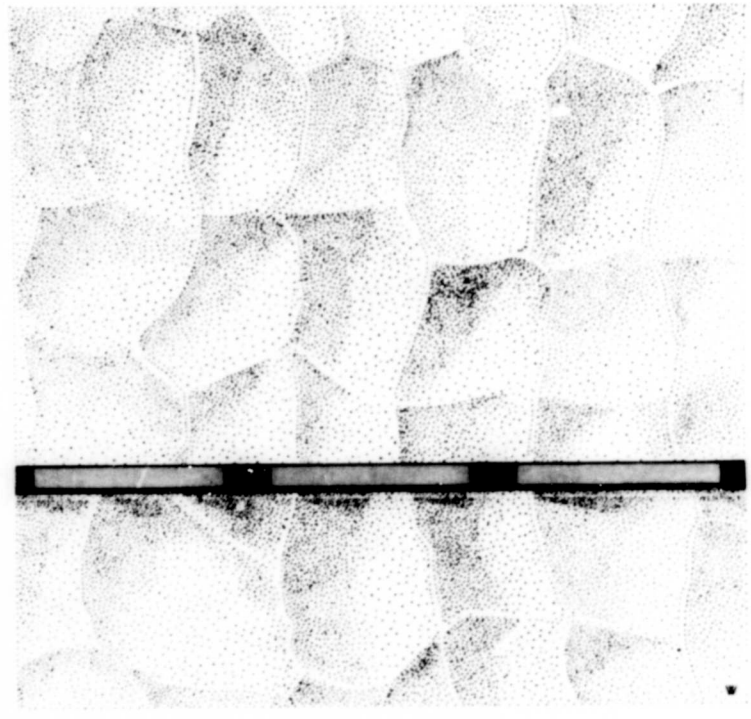

FIGURE 8. SHORT CRESTED RIPPLES (PATTERN 3). Ripples in fine sand at a depth of 52 ft on D range. (Appendix I C, 23 November 1953). Ripple profile is trochoidal. Scale division 0.5 ft. (Drawing of a photograph).

Sediment Sampling

During the ripple observations a sample of sand was obtained from the crests of the ripples, and in many cases from the ripple trough as well. The samples were labeled by date, number, and the letter C or T was appended to identify the sample with the ripple crest or trough. In addition to the routine sampling from the surface of the ripple crest and the trough, on two occasions examination of the structure of the sand under the crests and troughs was accomplished by lithifying a core of sand *in situ* with a polyester resin.

Because the study was concerned with water-transported sediments, hydraulic sizes, which are based on settling velocity were used in preference to sizes obtained by sieving. The sand-size fraction of the samples were analyzed with an Emery Settling Tube (Emery 1938, Poole et al. 1951). Material coarser than 1 millimeter was removed before the settling tube analysis, and then the weight percentage recombined after analysis into one cumulative frequency curve.

The particle-size distributions of the sediments were expressed in terms of phi measures (Inman, 1952) that serve as approximate graphic analogues to the moment measures commonly employed in statistics. The parameters used include the median diameter, a measure of standard deviation, and a measure of skewness. They are computed from three percentile diameters obtained from the cumulative size-frequency curve of the sediment and are defined as follows:

1) phi median diameter $Md_\phi = \phi_{50}$,

2) phi deviation measure $\sigma_\phi = 1/2\ (\phi_{84} - \phi_{16})$,

3) phi skewness measure $\alpha_\phi = \dfrac{M_\phi - Md_\phi}{\sigma_\phi}$,

where $\phi = -\log_2$ of the diameter in millimeters, $M_\phi = 1/2\ (\phi_{16} + \phi_{84})$ is the phi mean diameter, and ϕ_{16}, ϕ_{50}, and ϕ_{84} are the diameters in phi units corresponding to the 16th, 50th and 84th percentiles respectively of the cumulative weight-percent (coarser) curve. Since one phi unit is equivalent to one Wentworth division, the phi deviation measure gives the standard deviation of the sediment in terms of Wentworth units.

The graphic phi measures are tabulated in Appendix I through IV. For convenience in interpreting sand size, the median diameter is also tabulated in microns, using conversion tables compiled by Page (1955). The accuracy of measurement of the median diameter is about 0.02ϕ, which converts to about 2 microns for very fine sand and about 15 microns for coarse sand (Poole, et. al. 1951; Inman, 1953).

Wave Measurement

Wave height and period and the depth of water were measured from the boat during most ripple observations. Since it was not practical to use a conventional pressure type wave recorder, the trace from a recording fathometer was used in its place. A wave record of this type is reasonably accurate when used from small boats over flat bottoms. At times when fathograms were not available, visual observations of wave height and period were used, but reduction of this type of data was not attempted unless it appeared that a simple series of waves existed.

When available, a twenty-minute section of wave record was analyzed to obtain the wave period T, and the height H, of the significant wave, which is defined as the wave with the period and height of the average of the highest one-third waves. The significant wave period and height and the depth of water were used to compute the horizontal diameter of the orbit of a particle of water near the bottom, referred to hereafter as the orbital diameter d_o, and the maximum horizontal velocity, u_m*.

Although no great claim is made for accuracy in the wave computations, in general, it was found that the computed values for the wave period T, and the orbital diameter d_o, compared favorably with the period and orbital diameter observed near the bottom by the divers. Although it is difficult to measure velocity under water, the period of oscillation and the amount of displacement can be estimated with reasonable accuracy by a diver with a stop watch and a fixed point of reference.

Equations from the Airy wave theory were used in computing the orbital diameter and the maximum orbital velocity for observations well seaward of the surf zone. An adaptation of the solitary wave theory was used for orbital diameter and velocity computations when waves were near the surf zone. The conditions under which the Airy or solitary wave theory were used and the procedures for computing orbital diameter and velocity are described in detail in Appendix V.

Expression of Hydraulic Conditions

The work of Exner (1925) and von Karman (1947) indicated that the character of current ripples formed by unidirectional flow could be related to the velocity of flow. For shallow water, Anderson (1953) showed a correlation to exist between ripple wave length and the Froude number. Tsubaki, Kawasumi, and Yasutomi (1953) found that the dimensions of current ripples showed good correlation with Einstein's (1942) bed load function Ψ, which is related to the ratio of the weight of a sediment particle to the lift force acting on the particle by the flow.

The practical application of hydrodynamic principles to ripples generated by oscillatory flow is more obscure. Bagnold (1946) in his

* It is realized that computations based on the significant surface wave do not necessarily give the "significant" orbital velocity and diameter at the bottom; however, under the conditions taken here this was not considered to be critical.

experiments on ripples generated on a movable bed, showed that ripples of shortest wave length were proportional to the horizontal amplitude of oscillation of the bed. Later, Manohar (1955) using somewhat similar apparatus showed that a modification of the ψ function could be used to predict the character of his model ripples.

Thus, general considerations indicated the need for a measure of the intensity of flow and, since the motion was oscillatory, for a measure of the particle displacement. However, the spectrum of ocean waves is often broad, so that the probable error of predicting mean values of velocity and orbital diameters may be in error by as much as 50%. Also, there is no satisfactory procedure for calculating the stress exerted on the bottom by wave motion. Because of these facts it was decided to base the characterization of the hydraulic conditions on simple dimensionless ratios that could be obtained at the time of ripple observation. The intensity of flow was characterized by the relative velocity u_m/u_1, where u_m is the computed maximum horizontal velocity near the bottom, and u_1 is the limiting value for initiating motion in sand of a given size.[1] Since the relation between velocity and critical stress required to initiate motion was not clear, it was decided to arbitrarily use a value of $u_1 = 7u_*$ where u_* is the threshold or critical friction velocity (Inman 1949). The factor 7 was chosen because it gave a limiting velocity which was consistent although somewhat conservative in comparison with laboratory data of Menard (1950) and Manohar (1955). Their data and the relation of $u_1 = 7\,u_*$ is plotted against particle size in figure 9.

The displacement of a water particle relative to the ripples was obtained by the ratio of d_o/λ where d_o is the orbital diameter near the bottom computed for the significant waves and λ is the ripple wave length. A graph showing the relation of the relative velocity, u_m/u_1, to the relative displacement d_o/λ for all observations for which wave parameters were computed is shown in figure 10.

The hydraulic conditions were arbitrarily grouped into two general types on a basis of the relative velocity and the relative displacement (figure 10). Type I includes those conditions in which either or both ratios have a value less than 2, and type II includes those cases in which both ratios exceed a value of 2. Thus, type II indicates conditions in which the velocity is large compared to that required to initiate motion of the sand and the orbital diameter is large compared to the ripple wave length. On the other hand, the three types I indicate: Ic) conditions where the velocities are approximately the same order of magnitude as the limiting velocity for initiating sand movement, or Ib) that the orbital displacements are similar in magnitude to the ripple wave length, or Ia) both velocity and displacement are limiting. In addition, two extreme hydraulic conditions were noted: the condition in

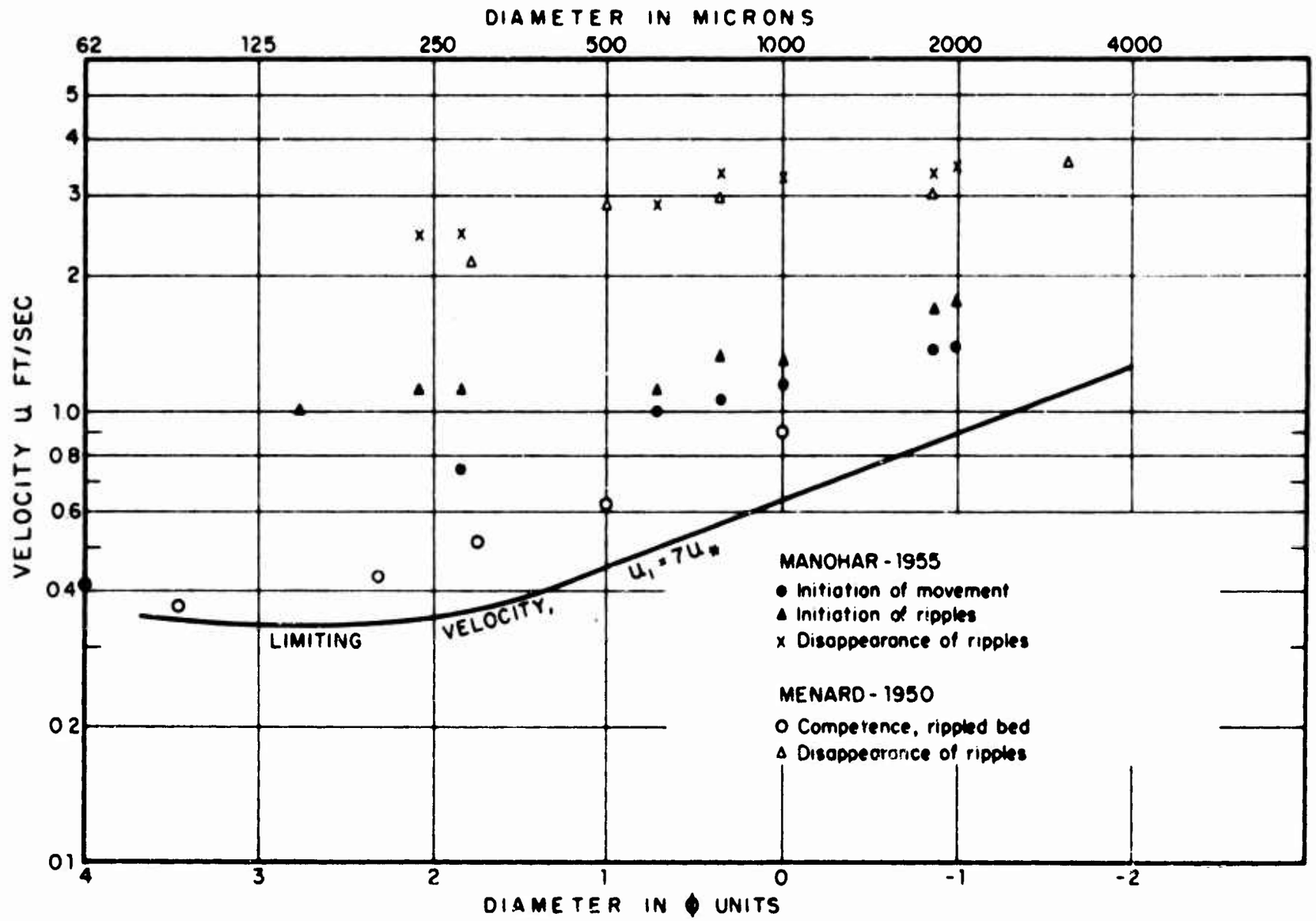

FIGURE 9. LIMITING OR MINIMUM VELOCITY FOR THE INITIATION OF MOTION OF SAND OF A GIVEN SIZE Limiting velocity, arbitrarily defined as equal to $7u_*$, where u_* is the threshold or critical friction velocity (Inman, 1949). For unidirectional flow this relation would give a limiting velocity equivalent, for example, to the mean velocity measured 1 ft above a bottom which has a roughness length of 2 cm Field observations near the surf zone indicate that planation and disappearance of ripples does not occur unless the maximum velocity associated with the wave crest somewhat exceeds that listed by Menard and Manohar.

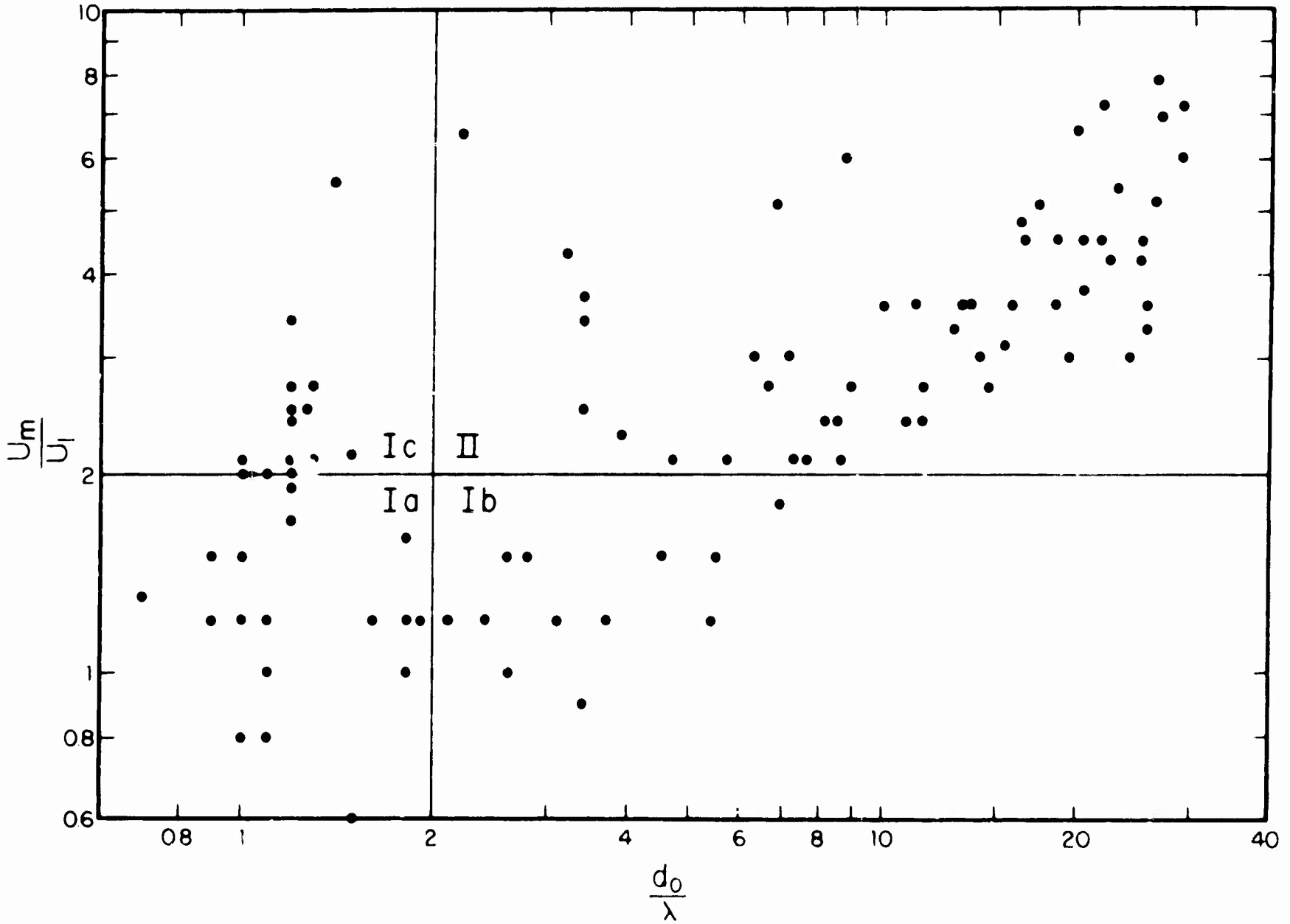

FIGURE 10. HYDRAULIC CONDITIONS EXPRESSED IN TERMS OF THE RELATIVE VELOCITY u_m/u_1, AND THE RELATIVE ORBITAL DIAMETER (DISPLACEMENT) OF A WATER PARTICLE NEAR THE RIPPLE. Type II indicates conditions in which both the orbital velocities and diameters are relatively large, while types I pertain to conditions where either or both the velocities or orbital diameters are limiting. The notation is defined in figures 1 and 9

which the velocity exceeded the upper limit for ripple formation and hence, the ripples were absent or "planed"; and the other extreme in which the water was still or "quiescent" and the ripple form was destroyed by burrowing organisms. The condition of planation was frequently observed near the surf zone while that of quiescence was more common in deeper water (figure 20).

INTERPRETATION

Sand ripples vary widely in size, shape, and duration. Some ripples are uniform with long parallel crests, others occur in various complex patterns such as rectangular, linguoid, and herringbone. Under some conditions ripples appear to change but little with time, while in others, especially near the surf zone, they are almost ephemeral in nature, changing with each wave surge. At times it appears that the ripples result from several factors, as for example when wave action is superimposed on tidal currents; at other times they appear to be in the process of modification from one form to another. Thus it becomes apparent that considerable care must be exercised in the collection of data if systemization is to be obtained from the various ripple forms, and the correlation of ripples and the forces generating them are to have significance. Therefore, care was taken to measure ripples in areas which were relatively far from bottom obstructions such as rocks, pier pilings, etc.

It is of course difficult in most cases to ascertain if the ripples measured were in fact formed by the waves present at the time of measurement. Many observers, dating back to Darwin (1883) and Forel (1895), have called attention to the fact that once formed, there is a tendency for the wave length of ripples to remain constant or to be but slowly modified, under changing conditions. In this regard, ripples in fine sand are more rapidly modified than ripples in coarse sand. A joint tabulation of ripple and wave characteristics was attempted only when it was considered that the ripples were in unison with the forces generating them. An exception to this undoubtedly occurred for measurements in coarse sand, as such ripples modify slowly and may only be in unison with generating forces under extreme wave conditions. Some aspects of complex ripples occurring near obstructions or in the process of modification are discussed briefly in a later section.

Sand and Ripple Size

The size of the sand is the single most important factor in determining the size of the ripple. A graph (figure 11) of the ripple wave length and the median diameter of the sand for all observations shows that in general, large ripples occur in coarse sand and smaller ripples in fine sand. It is also apparent from this graph that for equivalent sizes of sand, ripples from deeper water along exposed coasts tend to be larger than ripples in shallow water, and that ripples from areas such as bays and lakes where the wave fetch is limited have the shortest wave length

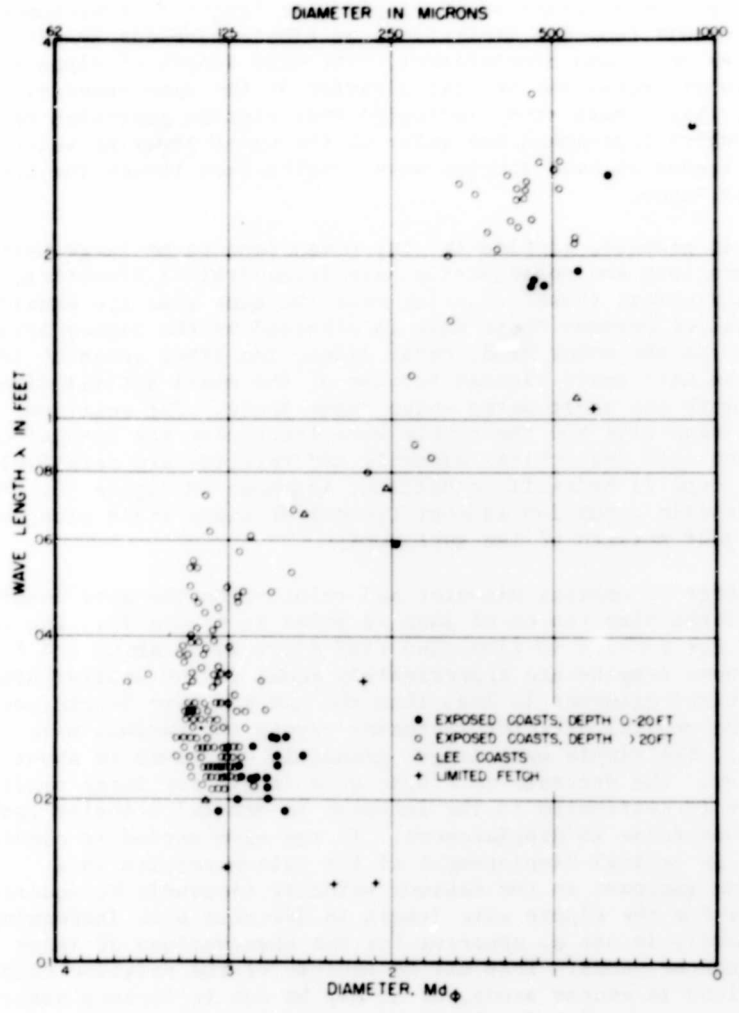

FIGURE 11. RIPPLE WAVE LENGTH AND SAND SIZE AT RIPPLE CREST. Includes all observations in which the median diameter of the sediment in the crest was 1000 microns or less. Tabulation of data is given in Appendix I through IV. Only data excluded is that for a ripple from a surge channel (Appendix II D), and for ripples generated by the re-formation of waves breaking over a barrier reef in the Hawaiian Islands (Appendix IV B, 8 December 1955).

of all. This general relation of ripple wave length to environment appears to result from the limitations on ripple size due to differences in orbital velocity and displacement. The wave length of ripples apparently cannot exceed the orbital diameter of the wave generating the ripple. Also, this study indicated that ripples generated by high velocities which approached the value of the upper limiting velocity (figure 9) tended to have shorter wave lengths even though the orbital diameter was large.

Thus, in general, ripples in the ocean tend to be large because the waves are long and consequently have large orbital diameters. Of these ocean ripples, those occurring near the surf zone are usually somewhat smaller because their size is affected by the higher orbital velocities. On the other hand, bays, lakes, and other areas of limited fetch tend to have small ripples because of the small orbital diameters associated with the short waves which occur there. The relation between the sand size and the ripple wave length for the special conditions where both the orbital diameter and velocity are relatively large, i.e. type II hydraulic condition, is shown in figure 12. The type II hydraulic condition is most typical of sandy areas along exposed coastlines just seaward of the surf zone.

The effect of orbital diameter and velocity on the wave length of ripples in three size ranges of sand is shown in figure 13. The maximum wave length for ripples in fine sand (125 microns) is about 3/4 foot. The ripple wave lengths are approximately equal to the orbital diameter, when the orbital diameter is less than the maximum wave length for the sand. As the orbital diameter increases beyond the maximum wave length of 3/4 foot., the ripple wave length gradually decreases to about 1/4 foot or less. The decrease in ripple wave length for large orbital displacement is attributed to the increase in orbital velocity rather than to the increase in displacement. If the wave period is constant, an increase in orbital displacement at the bottom results in a corresponding increase in the maximum velocity (Appendix V, equation 3). The tendency for the ripple wave length to decrease with increasing orbital velocity is not as apparent for the observations of large ripples in coarse sands. This may be because of the relative paucity of observations in coarse sands, or it may be due to factors associated with the wider range of hydraulic conditions and geographic location of the coarse sand stations. A tendency for ripple wave length to decrease near the upper critical velocity was not observed by Manohar (1955) in his laboratory studies of ripples generated on a movable bed.

Since the orbital diameter in shallow water is principally dependent on the wave height and period, on the average there exists a basic difference in wave length between ripples generated by wave action along oceanic coasts and those generated along the shores of water bodies with limited fetches such as small lakes. This dependence of ripples on the character of the waves generating them should be helpful in evaluating model studies of sand transport. It should also prove helpful in interpreting ancient environment from fossil ripple marks.

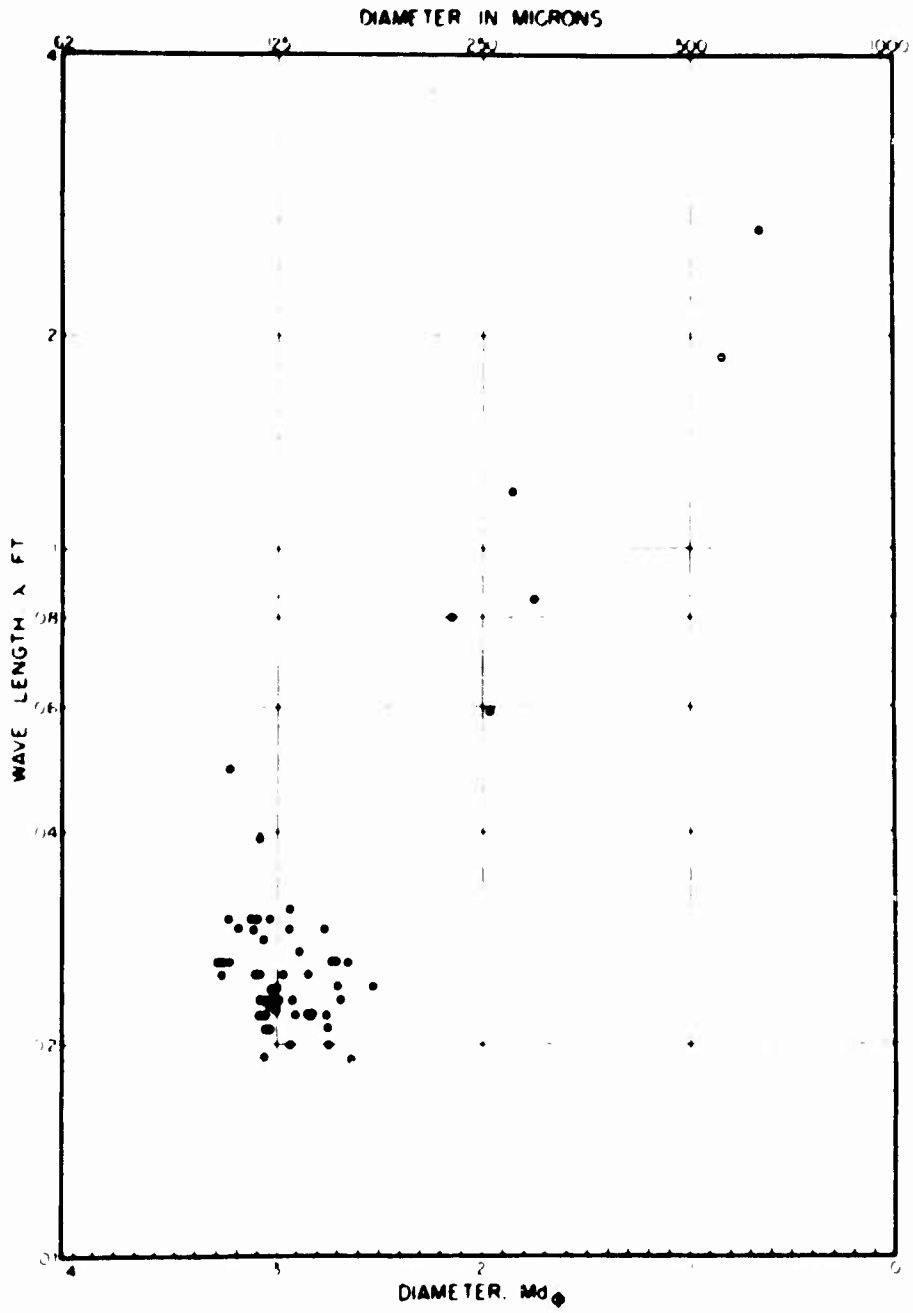

FIGURE 12. RIPPLE WAVE LENGTH AND SAND SIZE AT RIPPLE CREST Includes observations where both orbital diameter and maximum velocity are large (Type II hydraulic condition). These conditions are most typical of sandy bottoms near the surf zone of ocean beaches. This data is also plotted in figure 11. Hydraulic Conditions are defined in figure 10.

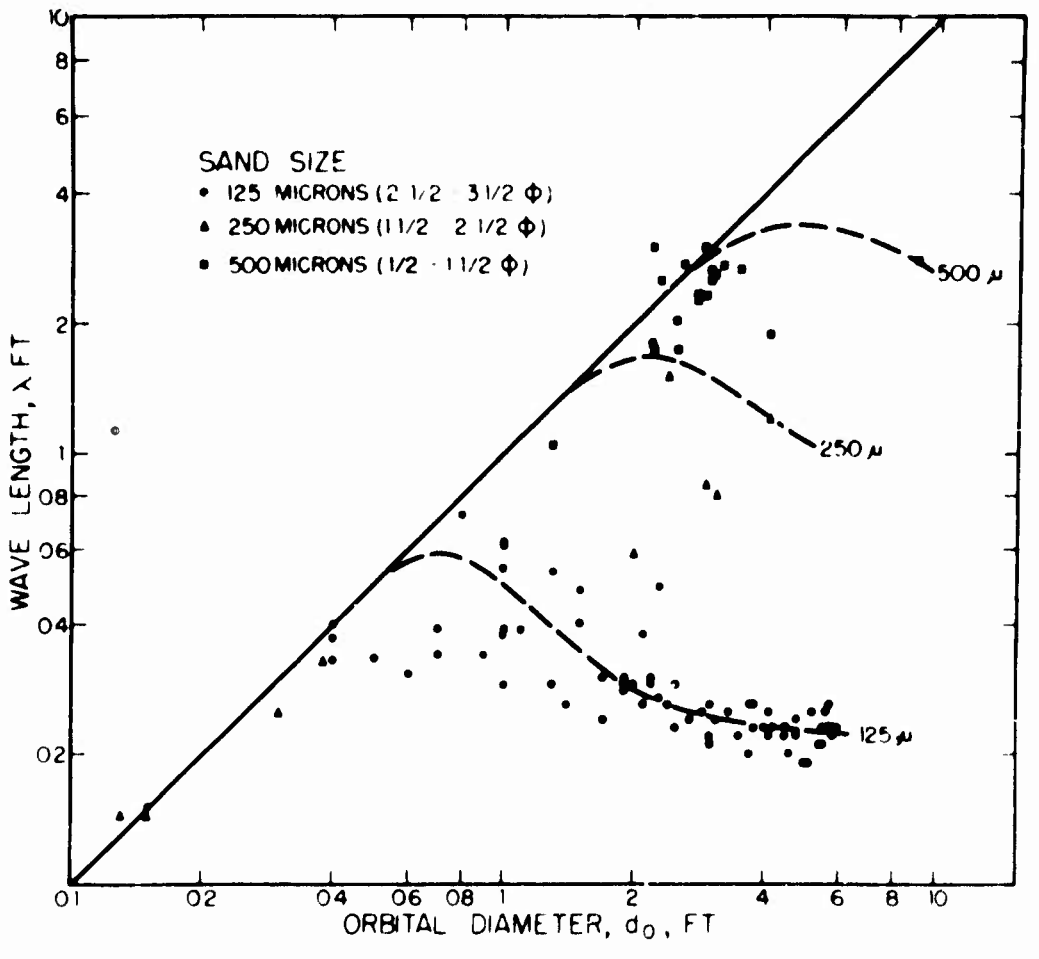

FIGURE 13. RELATION BETWEEN RIPPLE WAVE LENGTH AND THE ORBITAL DIAMETER OF WAVE MOTION FOR THREE RANGES OF SAND SIZE. The orbital diameter is a controlling factor in ripple wave length until the ripple reaches a maximum size. Increases in orbital diameter beyond the value of maximum wave length result in a decrease in ripple wave length, apparently because of the increase in the maximum orbital velocities. The orbital velocities for the 125-micron sand approach the disappearance or planation velocity at large orbital diameters (d_o greater than about 4 ft.). Because of the paucity of points for the coarser sands the dashed lines are intended to be more schematic than best fit.

Ripple Profiles

The ripple index λ/η which is the inverse of the steepness, averaged between 8 and 10 for fine and very fine sands and about 6 for coarser sands. The variation in ripple index for fine sands was great, ranging from about 5 to 20, while in coarser sands it was relatively constant (figure 14). Even for small wave lengths the index for medium and coarse sands fell within a range of $4\frac{1}{2}$ to 8. In part, the greater variability in fine sands results from the difficulties in measuring ripple heights discussed previously; however, there were sufficient observations to indicate that the difference is real and that the ripple index in fine sands can be much larger than in coarse sands. There is some correlation in fine sands between ripple index and the magnitude of the relative displacement at the bottom, d_o/λ, and relatively velocity u_m/u_1, which suggests that when the relative displacements and velocities are large, as near the surf zone, the ripples are less steep and thus have larger indices (figures 15 and 16). The plotted points in figure 16 for ripple index and relative velocity indicate a positive correlation for fine sand and little or no correlation for coarse sand.

The steepest ripples were commonly trochoidal in profile and were usually restricted to deeper water along exposed coasts and somewhat shallower water along lee and protected coasts (figure 5). The steep ripples are of the vortex type, the material on the ripple crest being lifted above the bottom and being moved an integral number of wave lengths with the passage of each wave crest and trough. Hydraulic condition Ia seems to be most conducive to the formation of ripples with steep trochoidal profiles. This condition occurs near the junction of the solid and dashed lines in figure 13 where the ripple wave lengths are greatest.

The solitary ripples which are most typical of fine sand in very shallow water tend to be less steep. The solitary ripples are formed when the wave trains are regular and the bottom velocities and the orbital diameters are relatively large, which is typically a Type II hydraulic condition. The higher velocities which are associated with the solitary profiles appear to place the material in a state of "sub-suspension" with the passage of each wave crest. In this case the bottom material is moved on and off shore as a thin but dense layer of suspended particles, and the discrete cloud of suspended particles which form at the crest of the trochoidal ripples appears to be absent. The thickness of the layer of "sub-suspension" although somewhat variable, is usually of the order of a few centimeters, and appears to depend on the size of the sand and on the orbital velocity and periodicity of the waves.

Sorting

The amount of sand available for transport was reflected in the relation between the size distribution of sand in the ripple crests and

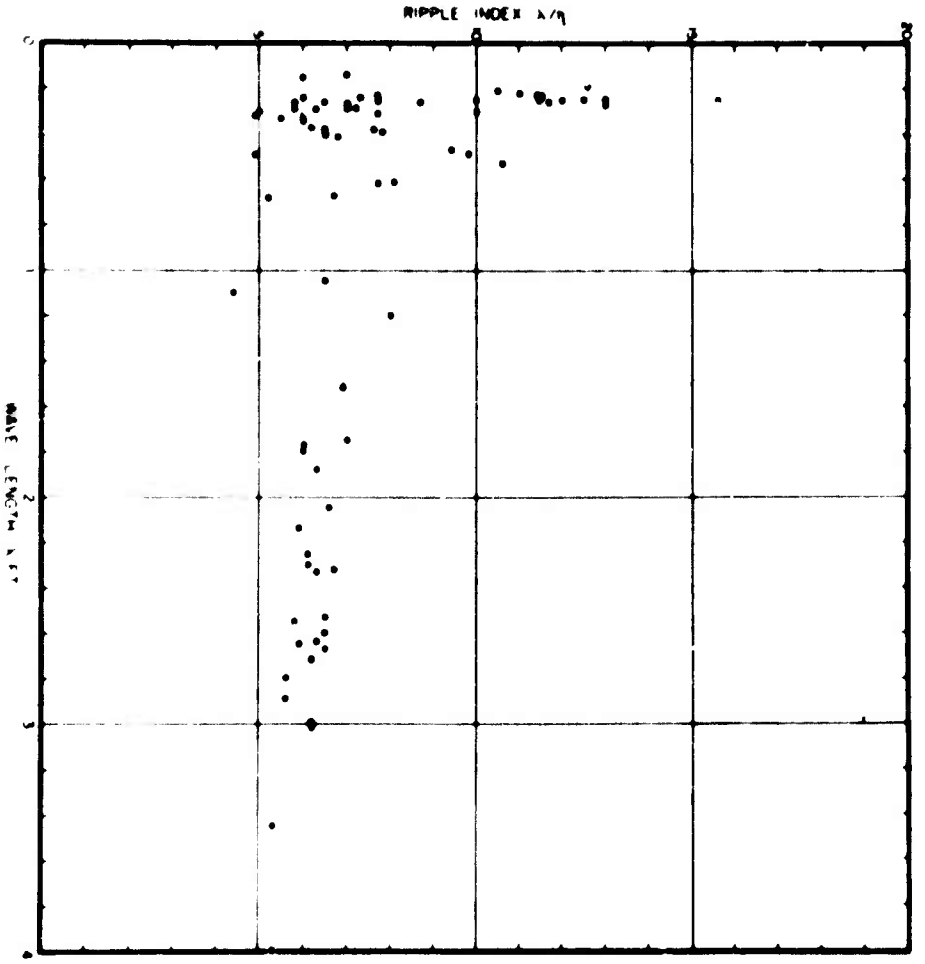

FIGURE 14 RELATION OF RIPPLE INDEX TO RIPPLE WAVE LENGTH FOR ALL OBSERVATIONS. (Ripple index is the inverse of ripple steepness.)

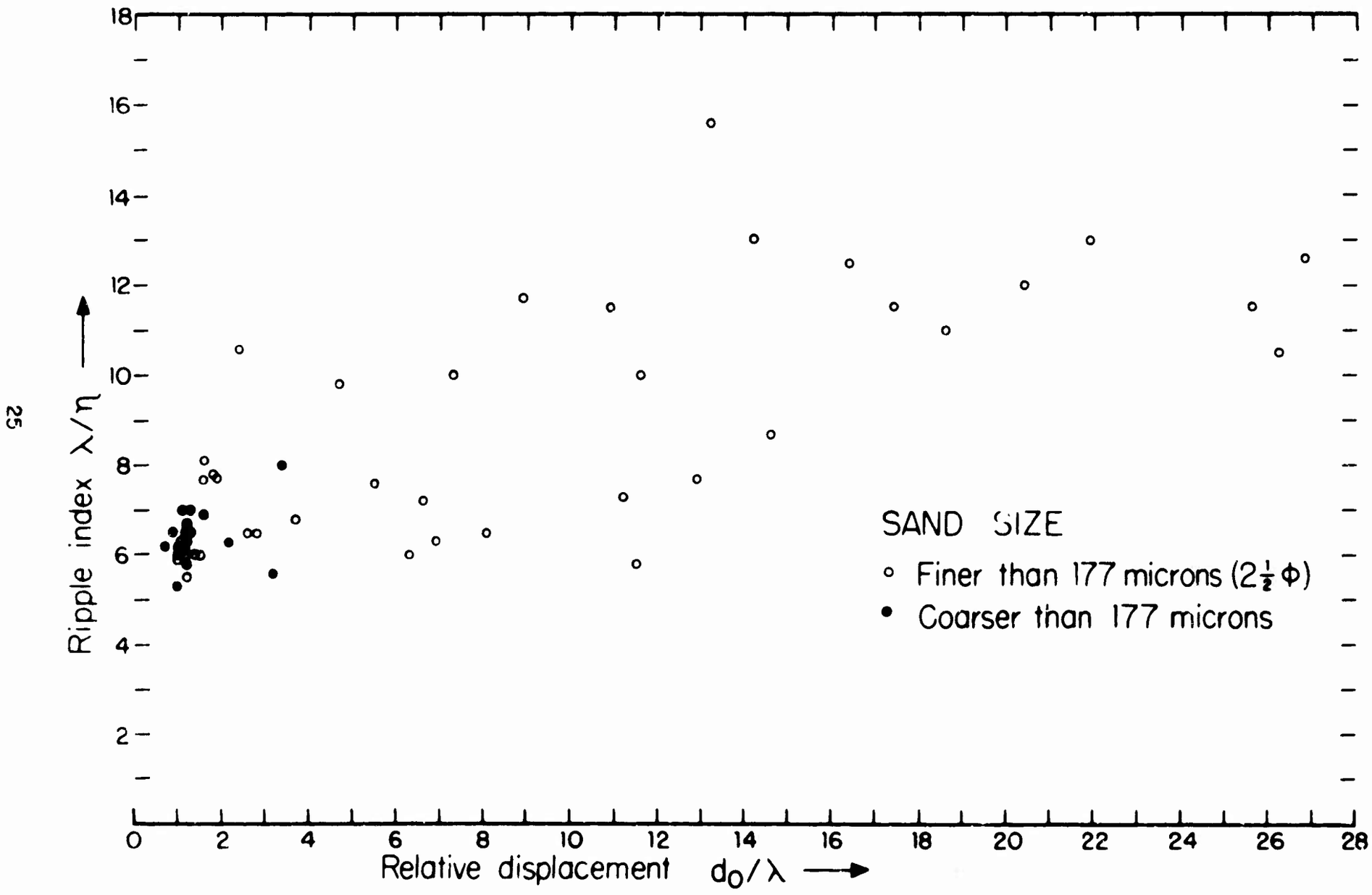

FIGURE 15 REATION BETWEEN RIPPLE INDEX AND RELATIVE DISPLACEMENT OF A WATER PARTICLE NEAR THE BOTTOM.

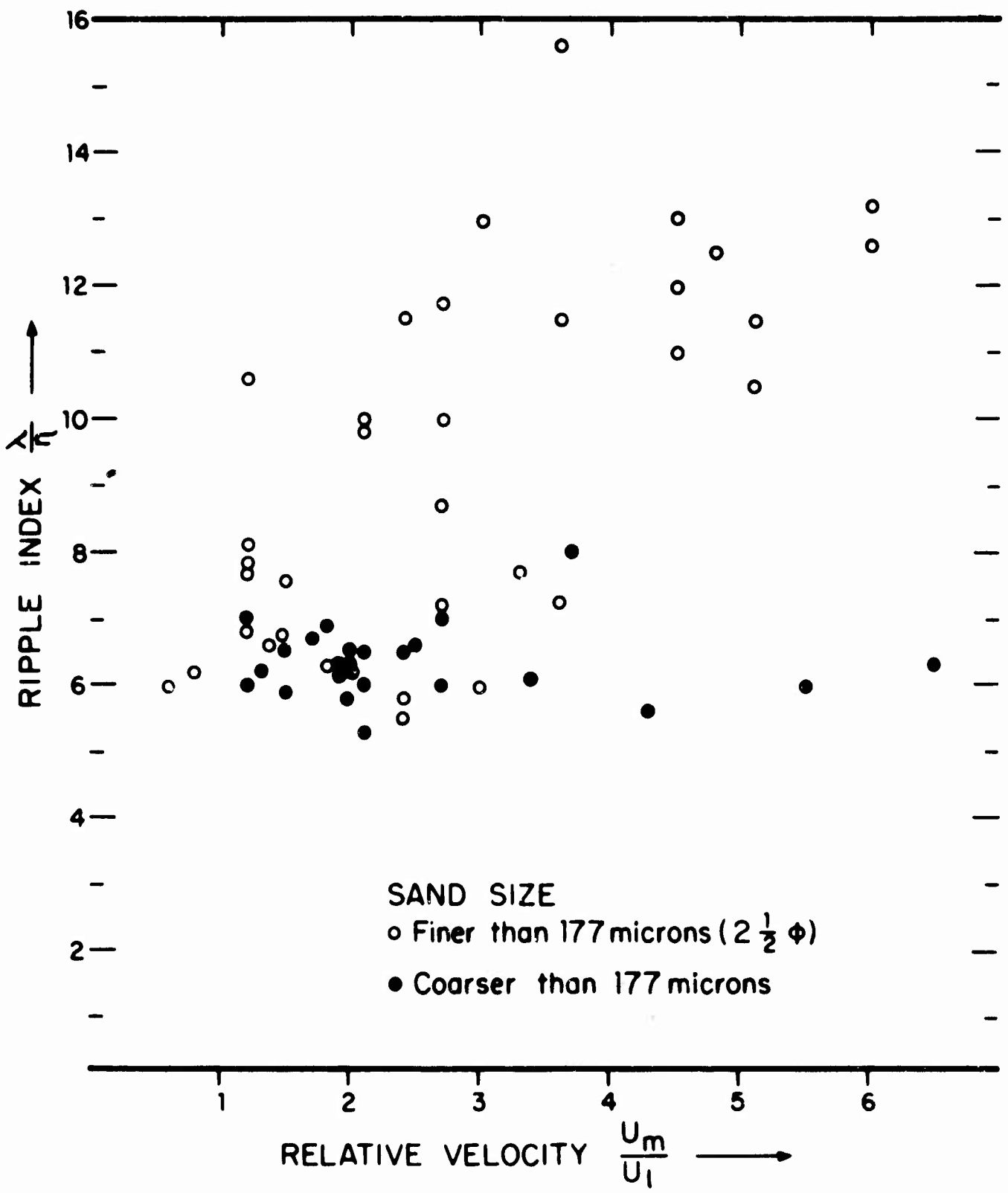

FIGURE 16. RELATION OF RIPPLE INDEX TO THE RELATIVE VELOCITY OF A WATER PARTICLE NEAR THE BOTTOM. A positive correlation is indicated for fine sands, while the index remains approximately constant for sands coarser than about 177 microns ($2\frac{1}{2}\phi$)

troughs. In general, if there was an abundance of sand available for transportation, the material of the largest size and least density was typically found on the ripple crests and the finest and heaviest material in the trough. If the source of sand was limited, a common condition along exposed rocky coasts, then the ripple crest consisted of sand sorted from the rocks and the trough material was essentially residual, which was frequently coarser than the material in the ripple crest (compare figures 5, 6 and 7 with 17). In either case it is the type of sand in the ripple crest which is influential in determining ripple properties, such as wave length and steepness.

The relation between the size distribution of sediments in the ripple crest and trough is shown in figures 18 and 19. Inspection of these figures shows that in general the sediments from the ripple crest tend to be coarser and have smaller distribution measures (i.e., be better sorted) than the sediments from the trough. Better sorting in the ripple crest was typical of all environments, as shown in the graph of figure 19 and illustrated by the ripple photograph in figure 17.

In only three cases was the material in the ripple trough found to be coarser than that in the crest (figure 18). In two of these, the samples were from rocky areas on exposed coasts where there was a very limited supply of sand, and the other was from a bay where the waves were relatively small.

Because turbulence and lift force are most intense at the crest of a ripple, only the coarsest of the transportable material is deposited there. Since coarser sand forms larger ripples, the ripple tends to grow in size commensurate with the coarsest material which the waves are capable of transporting. The capacity of a ripple to sort out and remove fine sand increases with ripple size, as the intensity of the vortex and lift forces increases with the length of the ripple. The fine material is placed in suspension by the vortex at the ripple crest, and either carried from the area or is deposited in the ripple trough.

It was found that boundaries between coarse and fine sand areas were sharp and well-defined. Apparently this is a natural result of the fact that large ripples grow at the expense of small ripples, and that once large ripples are formed, wave action tends to expel fine sand from the area. It was observed that the fineness of the trough sediment relative to the crest sediment could be used as an index of the proximity of fine sand areas. On the other hand, similarity in size of crest and trough material, or the occurrence of coarser material in the trough, indicated that the large ripples were more distant from fine sand areas.

Fine Sand Ripples, D-Range, La Jolla

The relatively large number of systematic observations at the four stations on D-range make it possible to describe the fine sand ripples

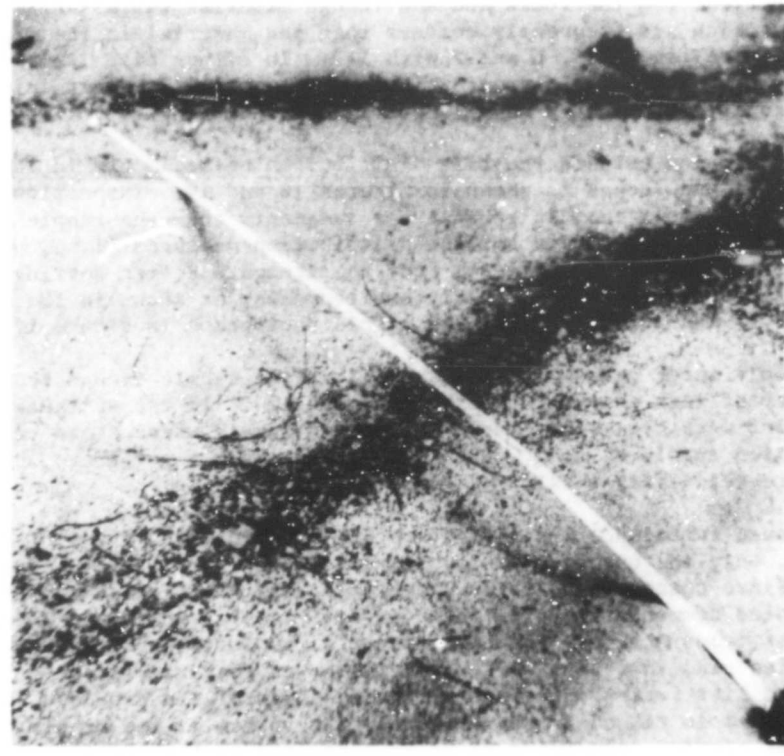

FIGURE 17. LARGE RIPPLE. Note coarse, poorly sorted debris in the trough and finer well sorted sand on the crest. Ripple is from a depth of 65 ft. off the rocky coast of Los Coronados Islands, Mexico, and has a wave length of 2.7 ft. Compare with ripple in figures 5, 6 and 7, which have coarsest sand on the ripple crests.

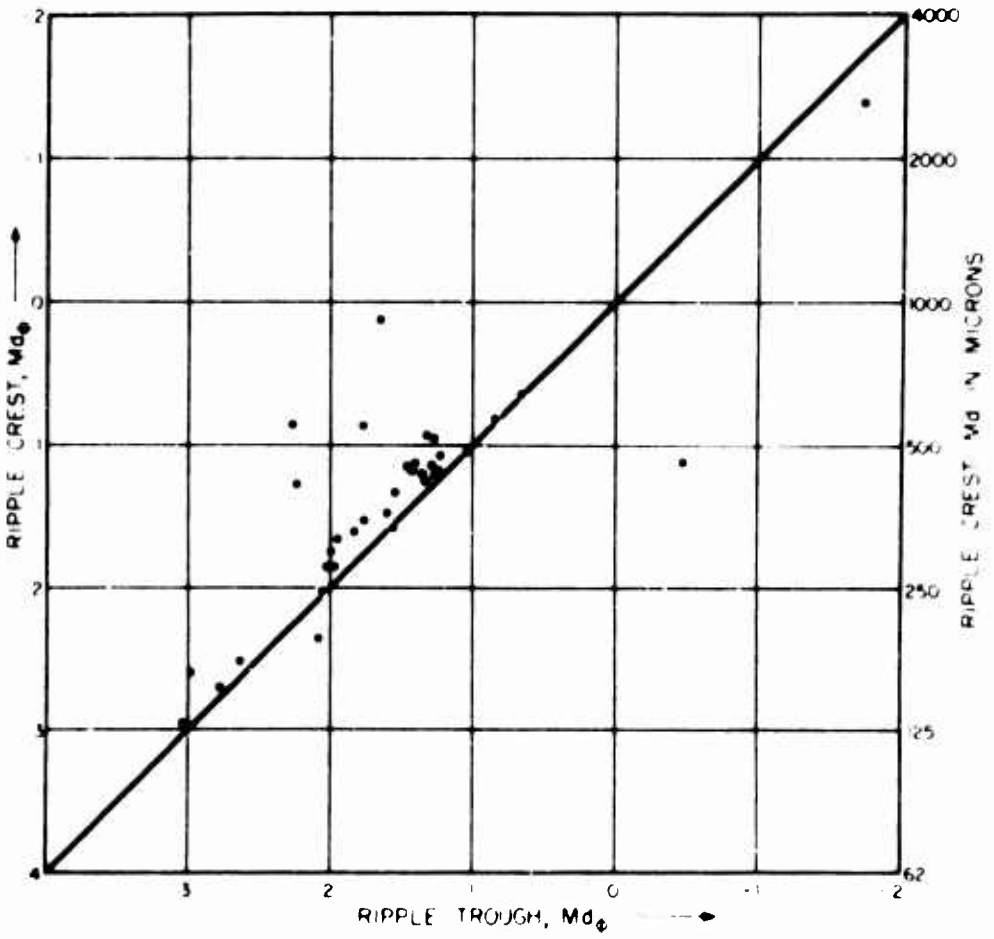

FIGURE 18. RELATION BETWEEN THE MEDIAN DIAMETER OF THE SEDIMENT IN THE RIPPLE CREST AND TROUGH. In general the crest sand is coarser than that in the trough. Exceptions occur in areas where the sand supply is limited and the sediment is relatively coarse compared with the ability of the waves to transport it. Two of the points below the line represent rocky areas with limited sand supply (Appendix II D, and III A, the other is from a small beach in Mission Bay (Appendix III A).

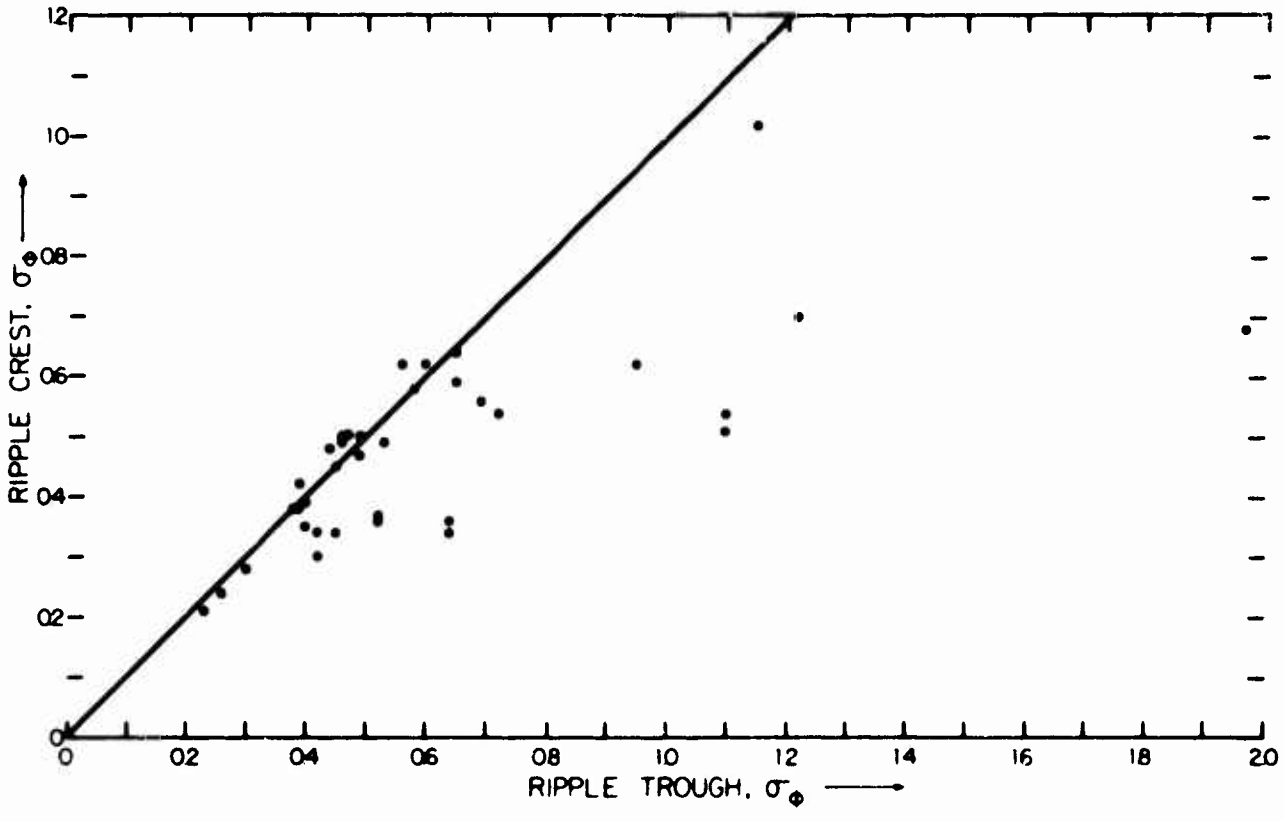

FIGURE 19. RELATION BETWEEN THE PHI DEVIATION MEASURE (SORTING) OF THE SEDIMENT IN THE RIPPLE CREST AND TROUGH. Sand from the crest was typically better sorted than that from the trough.

on this range in terms of depth and the frequency of occurrence of the various types of ripples. A complete presentation of these observations is given in Appendices I-a through I-D, and the data are summarized in tables 1 and 2, and presented graphically in figure 22.

Occurrence. Ripples were always present when the computed maximum orbital velocity was about 1/3 foot per second or greater. They were planed off and disappeared when the velocity exceeded about 2-1/2 feet per second. Because of high velocity, fine sand ripples were almost always absent in the breaker zone; they were frequently absent out to the depth of 18 feet, and occasionally at depths greater than 30 feet (Appendix I-B, 25 January 1955). Since orbital velocity decreases with increasing depth, the frequency of occurrence of periods during which the orbital velocity was insufficient to move sand was greater at the deeper stations. During these quiescent periods the ripple patterns were soon destroyed by burrowing organisms. Quiescent periods constituted 22% of the observations at a depth of 70 feet, and 5% at a depth of 50 feet (table 1). Although periods of quiescence certainly exist in shallow water as well, their occurrence is probably not statistically significant.

During quiescent periods, burrowing organisms and deposition of fine material from suspension give the bottom a very cluttered and dirty appearance as compared with the clean sand that appears when waves are actively forming ripples (compare figures 20 and 21). Within a matter of hours after sand ceases to move, the effect of bottom dwelling organisms in destroying ripples becomes apparent. Within a few days, as shown in figure 20, deposition of fine material causes the bottom to appear dirty and "rusty". Microscopic analyses of the film of "rusty" material covering the bottom on two occasions showed it to consist principally of siliceous planktonic diatoms.

The resumption of high orbital velocity following a period of quiescence soon causes the bottom to become rippled. The interaction of the wave motion and the ripples causes the fine material to be placed in suspension and the bottom soon appears to be composed of clean sand as shown in figure 21. The effective sorting action of the ripples must play an important role in removing silt- and clay-sized material from the bottom and in keeping it in suspension until it finds its way to deeper water.

Ripple Form. The patterns and profiles of the ripples varied systematically with depth (figure 22). In shallow water the fine sand ripples characteristically were long-crested (pattern 1), and were solitary in profile (figure 6). The only exceptions occurred in areas where the offshore flow of water in rip currents resulted in a confused water motion which caused the ripples to be intermediate or short-crested (patterns 2 and 3, illustrated in figures 7 and 8). Even in shallow water, short-crested ripples were more commonly associated with trochoidal rather than solitary profiles.

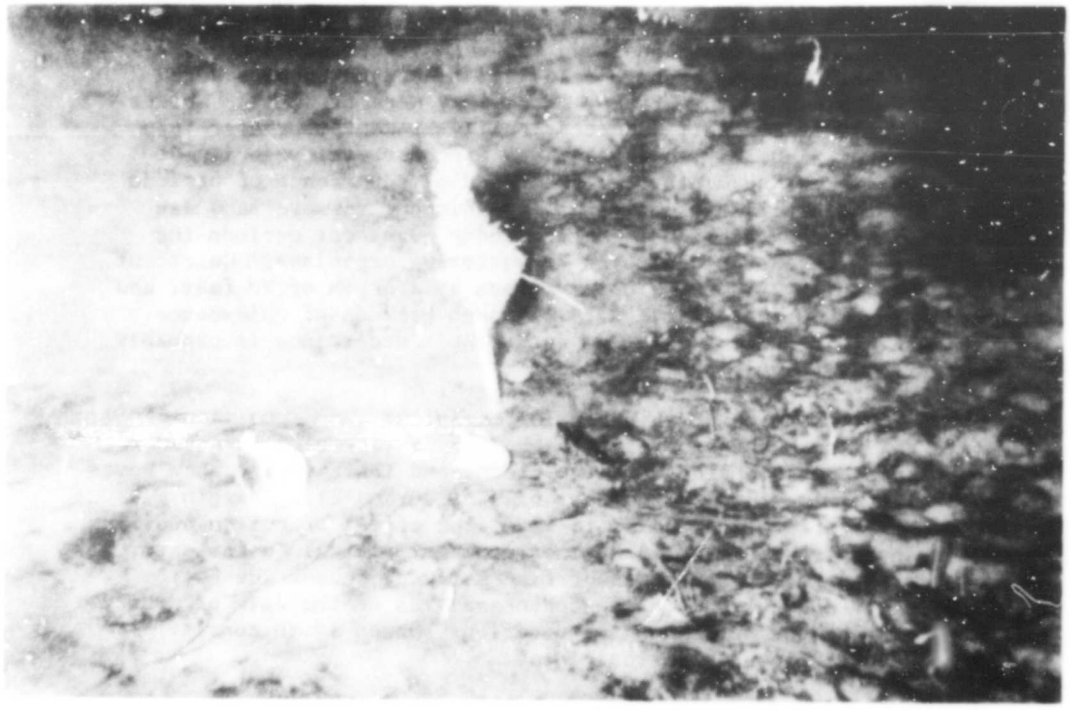

FIGURE 20. DEPOSITION OF MATERIAL FROM SUSPENSION AND DISRUPTION OF RIPPLE PATTERN BY BURROWING ORGANISMS DURING A QUIESCENT PERIOD ON D RANGE AT A 70 FT. DEPTH. (Appendix II D, 29 March 1954). Dark appearing material is principally deposition of planktonic diatoms. Compare with figure 21.

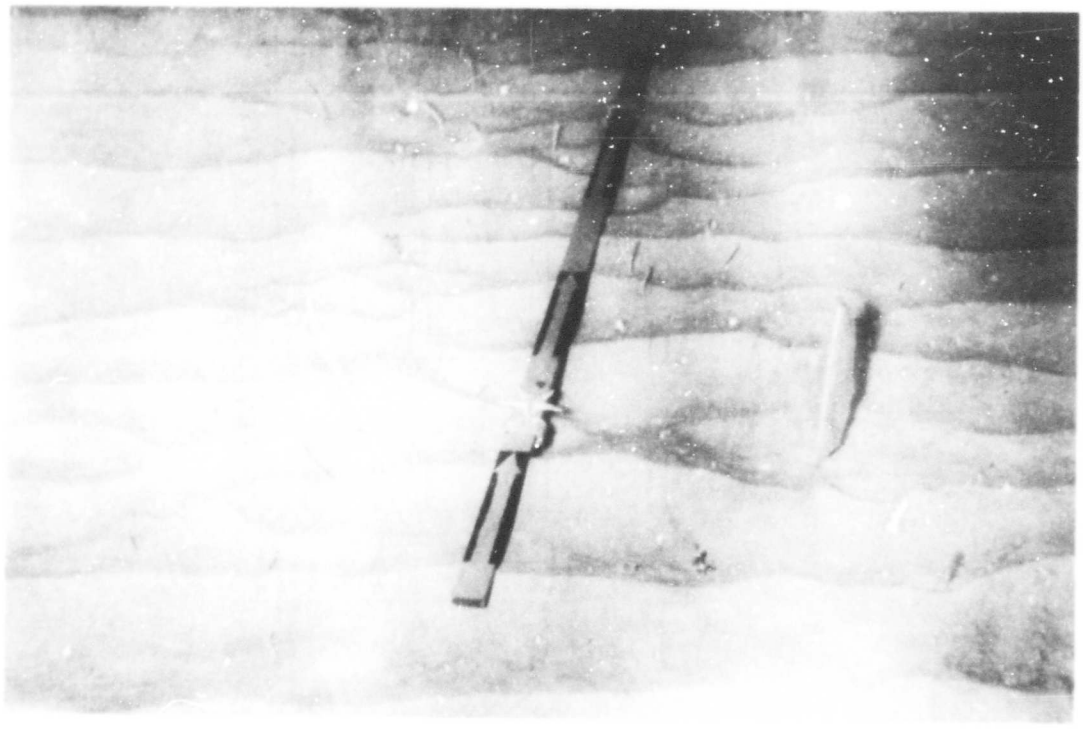

FIGURE 21 CLEAN RIPPLES GENERATED BY WAVE ACTION AT DEPTH OF 88 FT. ON D RANGE. Ripple profile is trochoidal and the wave length is 0.32 ft., (Appendix I D, 10 FEB 54). Note burrowing organisms; sea pen (right) and distal ends of brittle stars (grass-like protrusions) Each black or white divison is ½ ft; arrows point towards shore. Compare with figure 20.

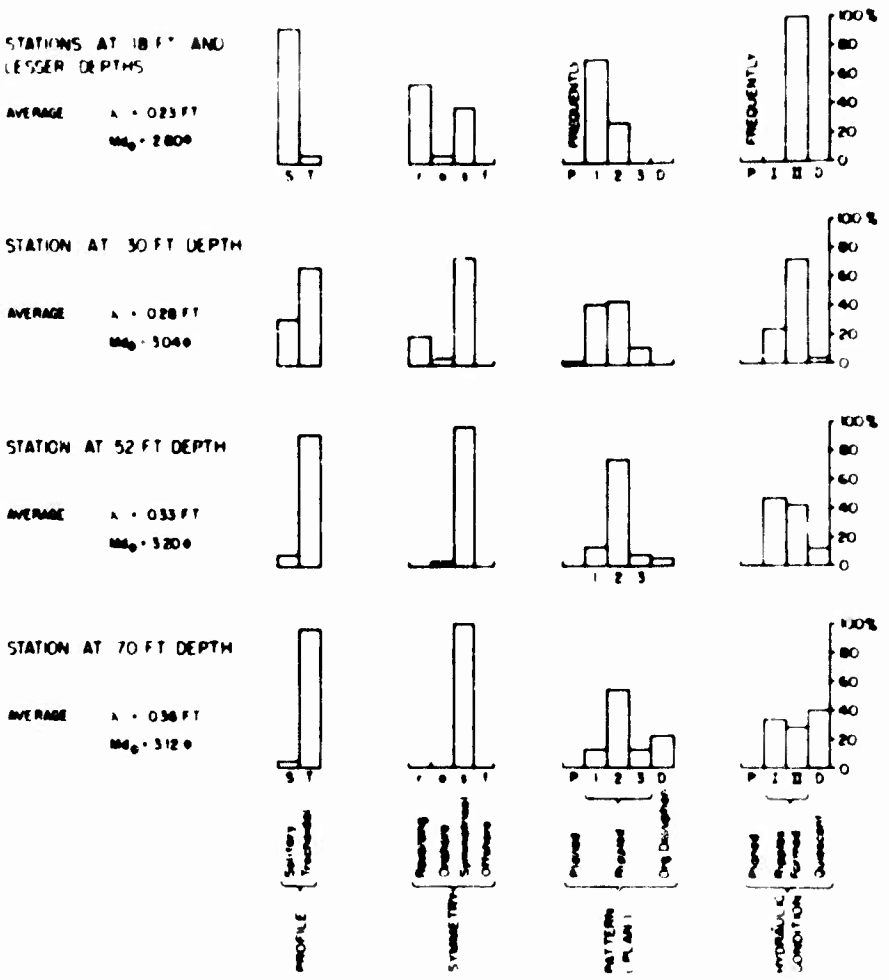

FIGURE 22. GRAPHIC SUMMARY OF RIPPLE PROPERTIES AT FOUR DEPTHS ON D RANGE, LA JOLLA, CALIFORNIA. Note that systematic difference occurs in the frequency of occurrence of all properties from shallow to deep water. Onshore and offshore symmetry pertains to asymmetrical profiles that resemble current ripples (lee face steep, stoss face gentle) formed by steady onshore or offshore flow respectively; reversing symmetry applies to conditions where ripple symmetry reverses with the passage of each wave crest and trough. Ripple patterns 1, 2, and 3 pertain to long, intermediate, and short crested ripples respectively, while planed refers to conditions where the orbital velocity was sufficiently great to cause ripples to disappear. Organic disruption of ripples occurs during quiescent conditions; other hydraulic conditions are defined in figure 10. Data are tabulated in Appendix I A through I D and are summarized in table I.

Table 1. Summary of ripple characteristics, D range, La Jolla. Individual observations are tabulated in Appendix 1A through 1D and the data are summarized graphically in figure 22.

STATION	18 ft. & lesser depths		30 ft. depth		52 ft. depth		70 ft. depth	
	No. of obs.	Value	No. of obs.	Value	No. of obs.	Value	No. of obs.	Value
RIPPLE WAVELENGTH								
Average	18	0.23 ft.	40	0.28 ft.	37	0.33 ft.	25	0.36 ft.
Maximum	1	.29 ft.	1	.21 ft.	1	.21 ft.	1	.22 ft.
Minimum	1	.19 ft.	1	.62 ft.	1	.72 ft.	1	.54 ft.
SAND SIZE								
Average Median Dia.	18	2.80 ϕ	40	3.04 ϕ	37	3.20 ϕ	25	3.12 ϕ
Coarsest " "		2.55 ϕ		2.80 ϕ		3.06 ϕ		3.28 ϕ
Finest " "		3.08 ϕ		3.28 ϕ		3.31 ϕ		2.90 ϕ
RIPPLE PROFILE								
Total Number Obs.	18		40		37		25	
Solitary	17	94%	13	32%	3	8%	1	4%
Trochoidal	1	6%	27	68%	34	92%	24	96%
RIPPLE SYMETRY								
Total Number Obs.	18		40		37		24	
Reversing	10	55%	8	20%	0	0%	0	0%
Onshore ($\beta/\lambda < .45$)	1	6%	2	5%	1	3%	0	0%
Sym ($.45 < \beta/\lambda < .55$)	7	39%	30	75%	36	97%	24	100%
Offshore ($.55 \leq \beta/\lambda$)	0	0%	0	0%	0	0%	0	0%
RIPPLE PATTERN								
Total Number Obs.	18		41		39		32	
Planed P	Frequently		1	2%	0	0%	0	0%
Long crested 1	13	72%	17	42%	4	10%	4	12%
Intermed. " 2	5	28%	18	44%	30	77%	17	54%
Short " 3	0	0%	5	12%	3	8%	4	12%
Disrupted by organisms D	0	0%	0	0%	2	5%	7	22%
HYDRAULIC CONDITIONS								
Total Number Obs.	18		25		17		18	
Quiescent D	0	0%	0	0%	2	12%	7	39%
(Ia	0	0%	3	12%	4	23%	1	5%
Ripples (Ib	0	0%	3	12%	3	18%	5	28%
Formed (Ic	0	0%	0	0 %	1	6%	0	0%
(II	18	100%	18	72%	7	41%	5	28%
Planed P	Frequently		1	4%	0	0%	0	0%

Table 2. Representative ripple measurements, D range, La Jolla

Date and Station depth	Wavelength λ	Crest to trough β	Height η
21 Oct 53	0.25 ft	0.10 ft	0.02 ft
Station at 18 ft	.23	.09	.02
(Pattern 1)	.26	.09	.03
	.26	.09	.02
	.23	.08	.005
	.26	.12	.015
	.27	.10	.02
Mean	0.251	0.095	.019
C.V.*	8%	17%	55%
21 Oct 53	0.25 ft	0.12 ft	0.01 ft
Station at 30 ft	.23	.11	.015
(Pattern 1)	.24	—	.02
	.25	.11	.03
	.20	.10	.025
	.23	.12	.02
	.24	.12	.015
	.19	.09	.015
Mean	0.228	0.110	0.018
C.V.*	11%	9%	40%
20 Oct 53	0.28 ft	0.14 ft	0.02 ft
Station at 52 ft	.25	.12	.015
(Pattern 2)	.24	.11	.015
	.24	.11	.015
	.28	.11	.015
	.27	.14	.015
	.20	.10	.015
Mean	0.251	0.119	0.0157
C.V.*	11%	5%	13%
16 Nov 53	0.21 ft	0.09 ft	0.020 ft
Station at 52 ft	.24	.11	.015
(Pattern 2)	.23	.10	.010
	.19	.10	.025
	.36	.10	.020
	.34	.12	.045
Mean	0.261	0.103	0.0224
C.V.*	25%	10%	59%
19 Nov 53	0.23 ft	—	—
Station at 52 ft	.24	0.11 ft	0.015 ft
(Pattern 1)	.20	.11	.015
	.21	.13	.015
	.26	.12	.020
	.22	.10	.015
	.23	.09	.013
Mean	0.227	0.11	0.0155
C.V.*	9%	13%	14%
23 Nov 53	0.35 ft	0.16 ft	0.09 ft
Station at 52 ft	.25	.13	.06
(Pattern 3)	.30	.16	.03
	.27	.15	.04
	.29	.15	.02
	.27	.15	—
Mean	0.288	0.15	0.048
C.V.*	12%	7%	50%
28 Dec 53	0.21 ft	0.13 ft	0.070 ft
Station at 70 ft	.32	.12	.055
(Pattern 3)	.24	.12	.070
	.25	.18	.030
	.24	.11	.030
	.30	.12	.020
Mean	0.26	0.13	0.0458
C.V.*	14%	17%	44%

*Coefficient of variation is the ratio of the standard deviation to the mean, expressed in percent.

At progressively deeper stations there was a consistent change in ripple profile from solitary to trochoidal in pattern. At depths of 70 feet and greater, 65% of the ripple profiles were trochoidal and 66% of the ripple patterns were intermediate or short-crested.

Insofar as profile and pattern are concerned, the ripples tend to imitate in miniature the particular waves which generate them. In deeper water where orbital velocities are lower and the wave profile is approximately trochoidal, the ripples tend to be trochoidal. In shallow water where the velocities are higher and wave forms are solitary, the ripples tend to be solitary. In deeper water, the direction spectrum of waves is broader and the resulting variation in the direction of orbital motion is reflected in shorter crested ripples. In shallow water, because of refraction, the direction spectrum of the waves is narrow, resulting in a narrow spectrum of orbital velocities which produce long-crested ripples. On the other hand, the form of the ripple differs from that of the waves generating it in that the ripple wave length and steepness are greater in deeper water than in shallow water (figures 11 and 22). The average ripple wave length was 0.36 foot at depths greater than 70 feet, and 0.23 foot near the surface zone, even though the sand in the shallow water was slightly coarser.

Variation in Form. Measurements along D-range showed that ripple characteristics such as wave length, height, and symmetry were relatively uniform at any one time within the area of measurement (table 2). The variation in ripple wave length was considerably less, about 13%, than the variation in height, which was about 37%. The coherency of measurement was somewhat better for long-crested ripples (pattern 1) than for shorter crested ripples, although even short-crested ripples gave fairly consistent wave lengths as shown by comparison of figure 8 with the individual measurements listed in table 2. The relatively large variation in ripple height is due in part to the difficulties in making accurate measures of small ripples, as discussed previously.

The data in table 2 for the station at a depth of 52 feet on 16 November 1953 is representative of the least consistent data obtained. In this case the grouping of ripple wave lengths around values of 0.22 and 0.35 foot suggests that the ripples were not in complete unison with the waves generating them.

Comparison With Model Experiments

In many ways the findings from the laboratory and field are in agreement; however, there are significant differences which are illustrated by the following comparison of the field observations with the model experiments of Manohar (1955) and Bagnold (1946). The experiments by both Manohar and Bagnold were conducted in still water by subjecting the sediment bed to simple harmonic motion in a horizontal plane, a procedure adopted because the large bottom displacements and

high orbital velocities typical of long waves in the ocean cannot be obtained in wave channels in the laboratory.

1) The maximum ripple wave length obtained in laboratory studies was somewhat less than that obtained in nature for the same size sand, even though the displacement of the movable bed exceeded the ripple wave length. For example, the maximum wave length obtained in quartz sand of about 1 mm diameter was approximately 0.7 foot in Bagnold's experiments, 1.0 foot in Manohar's work, and about 4 feet in the ocean.

2) For a given size sand, the longest ripple wave lengths in nature were observed in deeper water where the orbital velocities generating them were near the lower limit required for ripple formation. At higher velocities the wave lengths of natural ripples tended to decrease. In the laboratory investigations of Manohar, the longest ripples occurred at higher velocities just prior to the disappearance of ripples. Since these ripples were very low, it is possible that the occurrence of similar phenomena could not be detected in the field.

3) The ripple index for natural sands of all sizes ranged from about 5 to 20, while in medium and coarse sands the range was from 5 to 8. Bagnold's measurements compared favorably with the field observations. However, Manohar's observations which were made in medium and coarse sand had much larger indices, with an average value of about 20. The steepest ripples in Manohar's study had an index of 13.

COMPLEX RIPPLES

Ripples which form near obstructions such as rocks, pier pilings, and the like are frequently complex and do not always fall readily into the classifications used for the simple forms to which this paper is primarily devoted. It is also common to find that bottom dwelling animals may have an appreciable effect upon ripple form. This is particularly true of colonial animals such as sand dollars and polychaete worms like Owenia fusiformis.

A complex arrangement of ripples which has been observed near the end of Scripps Pier on several occasions will serve to emphasize the diversity of patterns possible in the vicinity of bottom obstructions (figure 23). The pattern observed apparently results from the superposition of two ripples systems. One system consists of the ordinary wave generated ripples which have wave lengths of about 1/4 foot, and ripple crests paralleling the wave crest. These are superimposed on large low ripples which form at angles of 30° to 60° with the long axis of the pier and have wave lengths of about 2-1/2 feet. Near the end of the pier where the water is deeper, the ordinary short ripples form

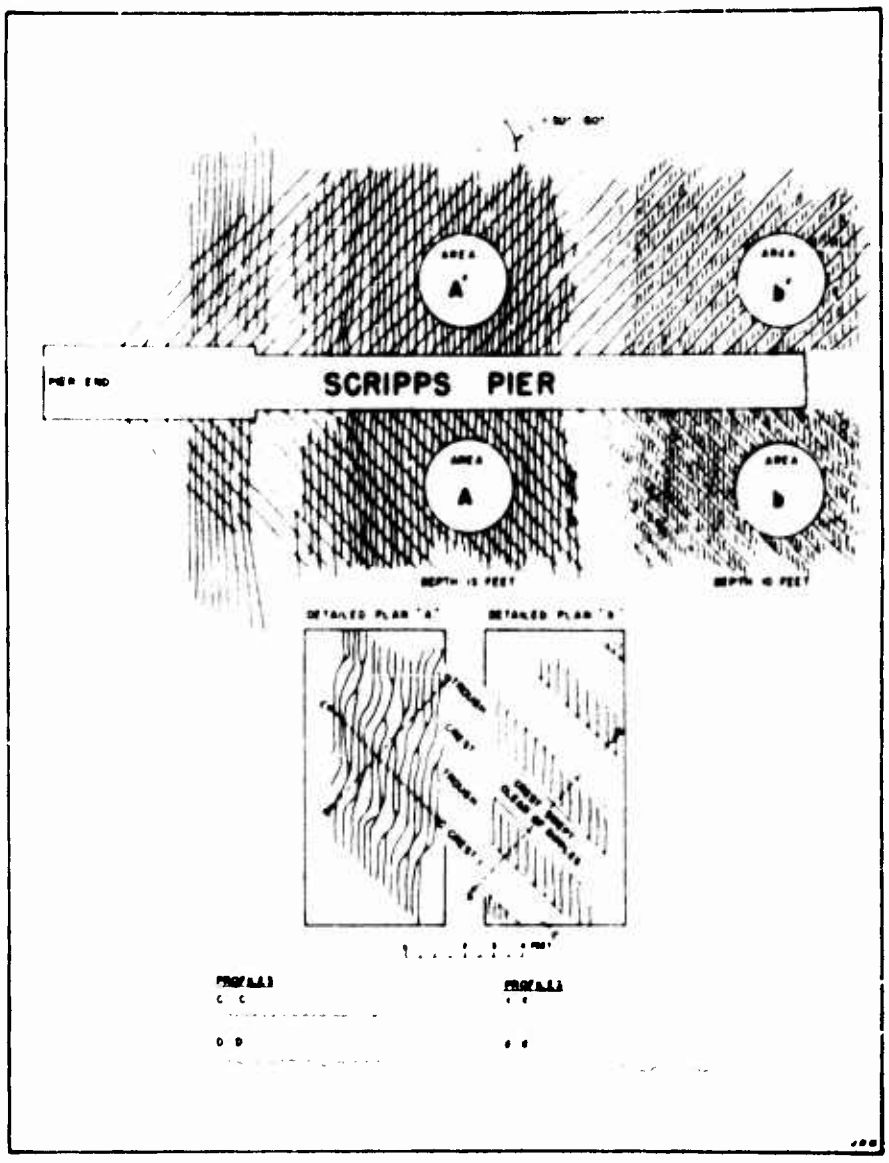

FIGURE 23 COMPLEX RIPPLE PATTERN OBSERVED AT THE OCEAN PIER OF THE SCRIPPS INSTITUTION OF OCEANOGRAPHY ON 30 DECEMBER 1954. The position of area "b" was observed to move off and on shore with groups of high and low waves

across the crests and troughs of the long ripple (area A, figure 23). In shallower water near the breaker zone, the ordinary ripples are planed from the crests of the large ripples by the high orbital velocities and are only found in the protective troughs of the large ripples (area b). The position of area b has been observed to move off and on shore with groups of higher and lower waves. On 30 December 1954, when the primary waves had a significant period of about 7 seconds and a direction of approach paralleling the axis of the pier, ripple patterns typical of area A were observed to occur in 10 feet of water when the waves were about two feet high, and to change to pattern b when the wave height increased to 3 or 4 feet.

ACKNOWLEDGMENTS

This paper represents in part results of research carried out by the University of California under contracts with the Beach Erosion Board and the Office of Naval Research. Field work was initiated in the summer of 1953 and the preliminary results were reported on briefly by Inman and Scott in 1954. The field phase of the study was largely the work of Earl Murray, who was in charge of the boat and took most of the underwater photographs and measurements. Assistance in analysis was given by Jean Short and Helene Flanders, and assistance with illustrations was given by Robert Winsett. Valuable suggestions and guidance during the study were contributed by Robert S. Arthur and Jeffery D. Frautschy.

LITERATURE CITED

Anderson, A. G.,1953. "Characteristics of sediment waves formed by flow in open channels", Proc. Third Midwestern Conference on Fluid Mechanics, University of Minnesota, pp. 379-95.

Bagnold, R. A. 1946. "Motion of waves in shallow water; interaction between waves and sand bottoms", Proc. Royal Soc. London, Vol.187, series A, pp. 1-15.

Bagnold, R. A. 1947. "Sand movement by waves: some small-scale experiments with sand of very low density", Jour. Inst. Civil Engineers, paper No. 5554, pp. 447-469.

Beach Erosion Board, 1954. "Shore protection planning and design", Corps of Engineers, Technical Report No. 4.

Darwin, G. H. 1883. "On the formation of ripple-marks in sand", Proceedings of the Royal Soc. of London, Vol. 36, pp. 18-43.

Einstein, H. A. 1942. "Formulas for transportation of bed load", Trans. Amer. Soc. Civil Engrs., Vol. 107, pp. 561-573.

Emery, K. O. 1938. "Rapid method of mechanical analysis of sands", Jour. Sed. Petrol. Vol. 8, pp. 105-111.

Exner, F. M. 1925. "Ueber die Wechselwirkung zwischen Wasser und Geschiebe in Flussen", Akad. d. Wiss., Wien, Sitzungsber. Math-Natur., Vol. 134:2a, pp. 165-203.

Forel, F. A. 1895. "Les rides de fond", Le Leman, Lausanne, Vol. 2, pp. 249-274.

Inman, D. L. 1949. "Sorting of sediments in the light of fluid mechanics", Jour. Sed. Petrol., Vol. 19, No. 2, pp. 51-70.

Inman, D. L. 1952. "Measures for describing the size distribution of sediments", Jour. Sed. Petrol., Vol. 22, pp. 125-145.

Inman, D. L. 1953. "Areal and seasonal variations in beach and near-shore sediments at La Jolla, California", Beach Erosion Board, Corps of Engineers, Tech. Memo. No. 39, 134 pp.

Inman, D. L. and N. Nasu. 1956. "Orbital velocity associated with wave action near the breaker zone", Beach Erosion Board, Corps of Engineers, Tech. Memo. No. 79, 43 pp.

Inman, D. L. and G. A. Rusnak. 1956. "Changes in sand level on the beach and shelf at La Jolla, California", Beach Erosion Board, Corps of Engineers, Tech. Memo No. 82, 30 pp.

Inman, D. L. and W. W. Scott. 1954. "Wave generated ripples in near-shore sands", Bull. Geol. Soc. Amer. Vol. 65, p. 1267.

Kindle, E. M. and E. M. Edwards. 1924. "Literature of ripplemarks", Pan-Amer. Geologist, Vol. 41, pp. 191-203.

Manohar, Madhav. 1955. "Mechanics of bottom sediment movement due to wave action", Beach Erosion Board, Corps of Engineers, Tech. Memo. No. 75, 121 pp.

Menard, H. W. 1950. "Sediment movement in relation to current velocity", Jour. Sed. Petrol., Vol. 20, pp. 148-160.

Munk, W. H. 1949. "The solitary wave theory and its application to surf problems", Ann. New York Acad. Sci., Vol. 51, Art. 3, pp. 376-424.

Page, H. G. 1955. "Phi-millimeter conversion table", Jour. Sed. Petrol., Vol. 25, pp. 285-292.

Poole, D. M., W. S. Butcher, and R. L. Fisher. 1951. "The use and accuracy of the Emery Settling Tube for sand analysis", Beach Erosion Board, Corps of Engineers, Tech. Memo. No. 23, 11 pp.

Tsubaki, T., T. Kawasumi, and T. Yasutomi. 1953. "On the influence of sand ripples upon sediment transport in open channels", Res. Inst. for Applied Mechanics, Kyushu Univ., Japan, Vol. 2, pp. 241-256.

van Straaten, L. M. J. U. 1953. "Rhythmic patterns on Dutch North Sea beaches", Overdruk uit Geologie en Mijnbouw, Nw. serie, Nr. 2, pp. 31-43.

von Karman, T. 1947. "Sand ripples in the desert", Amer. Technion Soc. Vol. 6, pp. 52-54.

APPENDIX IA - Exposed Coast, D Range, La Jolla, 18 ft. and lesser depths

1) Sample Date-Number	Median Diameter in Microns	2) Sediment Size Distribution Md_ϕ	σ_ϕ	α_ϕ	Depth of Water ft	Ripple Characteristics: Wave Length λ ft	Height η ft	Index $\frac{\lambda}{\eta}$	3) Symmetry β/λ	No. Meas.	4) Pattern	5) Profile	Waves: Period T sec	Orb. Diam. d_o ft	Orb. Veloc. u_m ft/sec	Hydraulic Condition: $\frac{d_o}{\lambda}$	$\frac{u_m}{u_1}$	6) Type
31 Aug 53-3	118	3.08	.41	-.12	10	.19	.015	12.6	r	5	1	S	10	5.1	2.0	26.8	6.0	II
7 Jul 54-1	130	2.94	.38	0	10	.23			r	7	1	S	10	5.5	2.4	23.9	7.2	II
7 Jul 54-2	132	2.92	.37	+.03	7	.22			r	6	1	S	10	5.8	2.6	26.3	7.8	II
27 Jul 54-1	136	2.88	.44	-.02	8	.22			r	11	1	S	10	4.8	2.4	21.8	7.2	II
27 Jul 54-2	129	2.95	.38	-.05	11	.20			r	8	1	S	10	4.6	1.8	23.0	5.4	II
27 Jul 54-3	145	2.79	.48	-.02	15	.22			r	7	2	S	10	4.5	1.4	20.5	4.2	II
2 Aug 54-1	171	2.55	.37	0	9	.24			r	14	1	S	10	4.8	2.2	20.0	6.6	II
2 Aug 54-2	139	2.85	.49	-.05	14	.22			r	15	1	S	10	3.0	1.2	13.6	3.6	II
2 Aug 54-3	157	2.67	.42	-.05	8	.19			r	15	1	S	10	5.0	2.3	26.3	6.9	II
17 Jul 53-1	153	2.71	.38	-.03	18	.24	.033	7.3	s	5	2	S	7	2.7	1.2	11.2	3.6	II

1) Samples from ripple trough designated by T, all others are from crest of ripple.

2) Size distribution expressed in graphic phi measures; Inman, 1952 (see text).

3) When not measured, symmetry determined by observation: r) reversing with each wave; s) symmetrical; o) asymmetrical, steep slope facing onshore; f) asymmetrical, steep slope facing offshore.

4) Pattern: 1) crest length greater than 8 λ; 2) crest length 3 λ to 8 λ; 3) crest length less than 3 λ.

5) Profile: S) solitary; T) trochoidal; SW) sawtooth.

6) Types I and II are defined in figure 10. P indicates surface of bottom smooth or planed because velocity exceeds upper critical limit for ripples; D refers to quiescent conditions where ripples were destroyed by burrowing organisms.

APPENDIX IA - Exposed Coast, D Range, La Jolla, 18 ft and lesser depths (cont.)

1) Sample Date-Number	Median Diameter in Microns	2) Sediment Size Distribution Md_ϕ	σ_ϕ	α_ϕ	Depth of Water ft	Ripple Characteristics: Wave Length λ ft	Height η ft	Index $\frac{\lambda}{\eta}$	3) Symmetry $\frac{\beta}{\lambda}$	No. Meas.	4) Pattern	5) Profile	Waves: Period T sec	Orb. Diam. d_o ft	Orb. Veloc. u_m ft/sec	Hydraulic Condition $\frac{d_o}{\lambda}$	$\frac{u_m}{u_1}$	6) Type
23 Jul 53-1	154	2.70	.38	-.05	18	.23	.02	11.5	s	12	1	S		4.0	1.7	17.4	5.1	II
-1T	146	2.78	.38	-.05														
12 Aug 53-1	146	2.78	.42	-.05	18	.20			o	13	1	S		3.7	1.2	18.5	3.6	II
14 Aug 53-1	145	2.79	.40	-.05	18	.29	.04	7.2	s	10	1	S	8	1.9	0.9	6.6	2.7	II
25 Aug 53-2	152	2.72	.45	0	18	.26	.04	6.5	.49	7	2	T	10	2.1	0.8	8.1	2.4	II
31 Aug 53-2	151	2.73	.42	-.07	18	.26	.02	13.0	s	8	2	S		3.7	1.0	14.2	3.0	II
11 Sep 53-2	147	2.77	.42	-.07	18	.21	.02	10.5	r	7	2	S	10	5.5	1.7	26.2	5.1	II
15 Oct 53-2	157	2.67	.38	-.03	18	.26	.02	13.0	.28	15	1	S	11	5.7	1.5	21.9	4.5	II
21 Oct 53-1	137	2.87	.45	-.09	18	.25	.02	12.5	.35	21	1	S	10	4.1	1.6	16.4	4.8	II

APPENDIX IB - Exposed Coast, D Range 30 ft

23 Jul 53-2	124	3.01	.46	-.06	30	.24	.03	7.7	o	10	1	S	9.2	3.1	1.1	12.9	3.3	II
27 Jul 53-1	117	3.09	.46	-.07	30	.28	.04	7.0	s	8	2	T	8	1.9	1.7	6.8	5.1	II
5 Aug 53-2	120	3.06	.47	-.11	30	.30	.05	6.0	s	7	3	T	6	1.9	1.0	6.3	3.0	II
12 Aug 53-2	117	3.10	.46	-.04	30	.39	.06	6.5	.58	6	2	T	6.2	1.1	0.5	2.8	1.5	Ib
21 Aug 53-2	118	3.08	.48	-.04	30	.22	.02	11.0	r	6	1	S	8.6	4.1	1.5	18.6	4.5	II

APPENDIX IB - Exposed Coast, D Range 30 ft (cont.)

1) Sample Date–Number	Median Diameter in Microns	2) Sediment Size Distribution Md_ϕ	σ_ϕ	α_ϕ	Depth of Water ft	Ripple Characteristics: Wave Length λ ft	Height η ft	Index $\frac{\lambda}{\eta}$	3) Symmetry $\frac{\beta}{\lambda}$	No. Meas.	4) Pattern	5) Profile	Waves: Period T sec	Orb. Diam. d_o ft	Orb. Veloc. u_m ft/sec	Hydraulic condition $\frac{d_o}{\lambda}$	$\frac{u_m}{u_1}$	6) Type
25 Aug 53–1	124	3.01	.48	-.02	30	.30	.03	10.0	.45	6	2	T	9.7	2.2	0.7	7.3	2.1	II
31 Aug 53–1	129	2.96	.47	-.04	30	.29	.045	6.3	.50	5	2½	T	10	2.0	0.6	6.9	1.8	Ib
15 Oct 53–1	126	2.99	.50	-.02	30	.25	.025	10.0	s	12	1	S	10.1	2.9	0.9	11.6	2.7	II
21 Oct 53–2	118	3.08	.48	-.17	30	.23	.02	11.5	.48	8	1	T	9.5	2.5	0.8	10.9	2.4	II
16 Nov 53–2	114	3.13	.47	-.17	30	.25	.02	12.0	r	7	1½	S	11.	5.1	1.5	20.4	4.5	II
28 Dec 53–2	117	3.10	.50	-.12	30	.23	.02	11.5	.50	8	1	T	13.	5.9	1.2	25.6	3.6	II
22 Jan 54–1	135	2.88	.47	-.02	30	.61	.075	8.1	.41	3	2	T	8.	1.0	0.4	1.6	1.2	Ia
2 Feb 54–1	124	3.01	.47	-.02	30	.25		10.0	r	6	1	S	13.	5.6	1.4	22.4	4.2	II
27 Apr 54–3	127	2.98	.51	-.06	30	.31	.04	7.7	s	6	2	T	5.	0.6	0.4	1.9	1.2	Ia
14 May 54–3	122	3.03	.45	-.07	30	.23			r	7	1	S	12.	5.8	1.5	25.2	4.5	II
18 Jun 54–3	121	3.05	.45	-.07	30	.23			s	7	1	S	8.	3.8	1.5	16.5	4.5	II
28 Jun 54–1	117	3.10	.51	0	30	.25			s	7	2	T						
26 Jul 54–1	117	3.10	.46	0	30	.34			s	5	3	T	5	0.7	0.4	2.1	1.2	Ib
16 Aug 54–1	121	3.05	.46	-.07	30	.30			s	6	3	T	7	1.7	0.7	5.7	2.1	II
26 Aug 54–1	115	3.12	.44	-.02	30	.28	.04	7.0	s	6	3	T						
1 Sep 54–1	118	3.08	.45	-.06	30	.42			s	4	3	T						
28 Sep 54–1	120	3.06	.45	0	30	.22			r	7	2	T						

APPENDIX IB - Exposed Coast, D Range 30 ft (cont.)

1) Sample Date-Number	Median Diameter in Microns	2) Sediment Size Distribution Md_ϕ	σ_ϕ	α_ϕ	Depth of Water ft	Ripple Characteristics: Wave Length λ ft	Height η ft	Index $\frac{\lambda}{\eta}$	3) Symmetry $\frac{\beta}{\lambda}$	No. Meas.	4) Pattern	5) Profile	Waves: Period T sec	Orb. Diam. d_o ft	Orb. Veloc. u_m ft/sec	Hydraulic Condition $\frac{d_o}{\lambda}$	$\frac{u_m}{u_1}$	6) Type
4 Oct 54-1	122	3.04	.47	-.10	30	.24			s	7	1½	S	6	1.7	1.0	7.1	3.0	II
15 Dec 54-3	118	3.08	.48	-.02	30	.21			s	7	2	T	10	3.0	1.0	14.3	3.0	II
20 Dec 54-1	138	2.86	.47	+.04	30	.22			s	13	1	S	15	4.5	1.0	20.4	3.0	II
21 Dec 54-4	125	3.00	.47	+.04	30	.23			s	6	1	S	11	4.2	1.2	18.3	3.6	II
25 Jan 55-3	103	3.28	.40	-.10	30	— (bottom flat; strong surge)							16	10.2	2.4		7.2	P
15 Feb 55-3	115	3.12	.48	-.12	30	.23			r	8	1	S						
10 Mar 55-3	129	2.96	.42	-.11	30	.22			s	7	2	T						
22 Mar 55-3	115	3.12	.50	-.04	30	.62	.08	7.7	s	3	2	T	8	1.0	0.4	1.6	1.2	Ia
6 Apr 55-3	113	3.14	.45	-.30	30	.25			o	6	2	T						
29 Apr 55-3	125	3.00	.45	-.04	30	.23			s	5	2	T						
5 May 55-3	129	2.95	.44	-.02	30	.25			s	7	2	T	Moderate surge					
17 May 55-2	122	3.03	.45	-.07	30	.22			s	6	2	T						
8 Jun 55-3	115	3.12	.40	-.05	30	.22			s	7	2	T						
6 Jul 55-3	122	3.03	.41	-.10	30	.23			r	7	1	S	9	5.7	2.0	8.7	6.0	II
1 Aug 55-3	144	2.80	.45	0	30	.33			s	5	2	T						
12 Oct 55-3	125	3.00	.42	+.05	30	.24			s	7	1	T						
23 Nov 55-3	113	3.14	.45	-.22	30	.22			r	8	1	S						

APPENDIX IB - Exposed Coast, D Range 30 ft (cont.)

1) Sample Date-Number	Median Diameter in Microns	2) Sediment Size Distribution Md_ϕ	σ_ϕ	α_ϕ	Depth of Water ft	Ripple Characteristics: Wave Length λ ft	Height η ft	Index $\frac{\lambda}{\eta}$	3) Symmetry β/λ	No. Meas.	4) Pattern	5) Profile	Waves: Period T sec	Orb. Diam. d_o ft	Orb. Veloc u_m ft/sec	Hydraulic Condition: $\frac{d_o}{\lambda}$	$\frac{u_m}{u_1}$	6) Type
13 Jan 56-3	127	2.98	.50	-.04	30	.23			s	8	2	T						
30 Jan 56-3	109	3.20	.48	-.30	30	.25			s	6	1	T						

APPENDIX IC - Exposed Coast, D Range 52 ft

10 Jul 53-1	106	3.24	.39	-.15	52	.39	.05	7.8	.55	7	2	T	6½	0.7	0.4	1.8	1.2	Ia
5 Aug 53-1	107	3.23	.42	-.12	52	.33	.06	5.5	.54	9	2	T	6	0.4	0.8	1.2	2.4	Ic
20 Oct 53-1	102	3.29	.38	-.13	52	.25	.016	15.6	.48	7	2	S	10.4	3.3	1.2	13.2	3.6	II
16 Nov 53-1	102	3.29	.38	-.08	52	.26	.022	11.7	.40	6	2	S	8.5	2.4	0.9	8.9	2.7	II
19 Nov 53-2	106	3.24	.38	-.05	52	.23	.02	11.5	.48	7	1	T						
23 Nov 53-1	103	3.28	.37	-.10	52	.29	.05	5.8	.51	6	3	T	(confused short crested)					
28 Dec 53-1	102	3.30	.36	-.17	52	.26	.03	8.7	s	7	2	T	13	3.8	0.9	14.6	2.7	II
14 Jan 54	105	3.25	.42	-.14	52	.24	.04	6.0	s	7	2	T						
28 Jan 54-2	106	3.24	.38	-.10	52	.53	.05	10.6	.51	3	2	T	9½	1.3	0.4	2.4	1.2	Ib
29 Mar 54-2	107	3.23	.41	-.10	52	.40			s	6	3	T	5	0.4	0.25	1.0	0.8	Ia
27 Apr 54-2	107	3.22	.40	-.05	52	.47	.05	9.4	s	4	2	T						
14 May 54-2	109	3.20	.40	-.05	52	.29			s	6	2	T	12	2.5	0.7	8.6	2.1	II
18 Jun 54-2	104	3.26	.38	-.10	52	.30			s	5	2	T	8	3.0	1.2	10.0	3.6	II

APPENDIX IC - Exposed Coast, D Range 52 ft (cont.)

1) Sample Date-Number	Median Diameter in Microns	2) Sediment Size Distribution Md_ϕ	σ_ϕ	α_ϕ	Depth of Water ft	Ripple Characteristics: Wave Length λ ft	Height η ft	Index $\frac{\lambda}{\eta}$	3) Symmetry $\frac{\beta}{\lambda}$	No. Meas.	4) Pattern	5) Profile	Waves: Period T sec	Orb. Diam. d_o ft	Orb. Veloc. u_m ft/sec	Hydraulic Condition $\frac{d_o}{\lambda}$	$\frac{u_m}{u_1}$	6) Type
28 Jun 54-2	107	3.23	.45	-.20	52	.22			s	7	2	T						
26 Jul 54-2	103	3.28	.39	-.10	52	.37	.06	6.2	s	4	2	T	5	0.4	0.25	1.1	0.8	Ia
16 Aug 54-2	107	3.23	.41	-.14	52	.29			s	5	2	T	8	1.3	0.5	4.5	1.5	Ib
26 Aug 54-2	107	3.22	.41	-.07	52	.28			s	5	3	T						
1 Sep 54-2	102	3.30	.40	-.15	52	.37			s	4	2	T						
28 Sep 54-2	108	3.21	.42	0	52	.28			s	6	2	T						
28 Sep 54-2	108	3.21	.42	0	52	.28			s	6	2	T						
4 Oct 54-2	101	3.31	.37	-.10	52	.24			s	7	2½	T						
15 Dec 54-2	109	3.20	.38	-.13	52	.26			s	6	2	T	10	1.4	0.4	5.4	1.2	Ib
25 Jan 55-2	120	3.06	.46	-.04	52	.21			s	5	1	S	16	5.4	1.1	25.7	3.3	II
15 Feb 55-2	113	3.14	.48	-.04	52	.23			s	8	2	T						
10 Mar 55-2	107	3.22	.43	-.11	52	.29			s	6	2	T						
22 Mar 55-2	112	3.16	.47	-.10	52	—							8	0.6	0.2		0.6	D
6 Apr 55-2	106	3.24	.36	-.35	52	.34			s	4	2	T						
29 Apr 55-2	109	3.20	.40	-.10	52	—												D
5 May 55-2	130	2.94	.54	0	52	.57			s	3	2	T	slight surge					

APPENDIX IC - Exposed Coast, D Range 52 ft (cont.)

1) Sample Date-Number	Median Diameter in Microns	2) Sediment Size Distribution Md_ϕ	σ_ϕ	α_ϕ	Depth of Water ft	Ripple Characteristics: Wave Length λ ft	Height η ft	Index $\frac{\lambda}{\eta}$	3) Symmetry $\frac{\beta}{\lambda}$	No. Meas.	4) Pattern	5) Profile	Waves: Period T sec	Orb. Diam. d_o ft	Orb. Veloc. u_m ft/sec	Hydraulic Condition $\frac{d_{50}}{\lambda}$	$\frac{u_m}{u_1}$	6) Type
17 May 55-1	117	3.09	.45	-.07	52	.33			s	5	2	T						
8 Jun 55-2	113	3.15	.38	-.03	52	.25			s	5	2	T						
6 Jul 55-2	117	3.10	.39	-.30	52	.22			s	7	1	T	9	3.5	1.2	15.9	3.6	II
1 Aug 55-2	110	3.19	.34	0	52	.24			s	7	2	T						
10 Sep 55-2	109	3.20	.34	-.12	52	.46			s	4	2	T						
3 Oct 55-2	113	3.15	.36	-.08	52	.72			o	4	2	T	7	0.8	0.35	1.1	1.0	Ia
12 Oct 55-2	102	3.29	.37	-.16	52	.36			s	5	2	T						
23 Nov 55-2	105	3.25	.38	-.13	52	.28			s	6	2	T						
13 Jan 56-2	118	3.08	.42	-.10	52	.45			s	4	1	T						
30 Jan 56-2	117	3.10	.36	-.08	52	.27			s	6	2	T						

APPENDIX ID - Exposed Coast, D Range 70 ft and greater depths

22 Jul 53-1	109	3.20	.38	-.10	70	.39	.06	6.5	.53	7	2½	T	13	1.0	0.5	2.6	1.5	Ib
28 Dec 53-3	106	3.24	.39	-.08	70	.26	.045	5.8	.50	6	3	T	13	3.0	0.8	11.5	2.4	II
26 Jan 54-1	106	3.24	.38	-.13	70	.49	.05	9.8	.41	4	2	T	10	2.3	0.7	4.7	2.1	II
27 Jan 54-1	109	3.20	.44	-.05	70	.41	.06	6.8		4	2	T	12	1.5	0.4	3.7	1.2	Ib
28 Jan 54-1	107	3.23	.38	-.08	70	.54			s	4	2	T	9½	1.0	0.35	1.8	1.0	Ia

APPENDIX ID - Exposed Coast, D Range 70 ft and greater depths

1) Sample Date-Number	Median Diameter in Microns	2) Sediment Size Distribution Md_ϕ	σ_ϕ	α_ϕ	Depth of Water ft	Ripple Characteristics: Wave Length λ ft	Height η ft	Index $\frac{\lambda}{\eta}$	3) Symmetry $\frac{\beta}{\lambda}$	No. Meas.	4) Pattern	5) Profile	Waves: Period T sec	Orb. Diam. d_o ft	Orb. Veloc. u_m ft/sec	Hydraulic Condition $\frac{d_o}{\lambda}$	$\frac{u_m}{u_1}$	6) Type
29 Mar 54-1	111	3.17	.42	-.17	70	—							5	0.2	0.1		0.3	D
27 Apr 54-1	117	3.10	.42	-.10	70	.41	.02	20.0	s	9	2	T						
14 May 54-1	113	3.15	.41	-.02	70	.38	.05	7.6	s	5	2	T	12	2.1	0.5	5.5	1.5	Ib
18 Jun 54-1	114	3.13	.38	-.03	70	.29			s	5	1	T	8	2.2	0.7	7.6	2.1	II
26 Jul 54-3	109	3.20	.40	-.12	70	—							5	0	0			D
16 Aug 54-3	111	3.17	.34	-.03	70	—							8	still				D
26 Aug 54-3	112	3.16	.42	-.09	70	—								still				D
1 Sep 54-3	110	3.18	.40	-.05	70	—								still				D
4 Oct 54-3	111	3.17	.42	-.18	70	.37			s	5	2	T						
15 Dec 54-1	105	3.25	.42	-.07	70	.29			s	6	2	T	10	1.0	0.3	3.4	0.9	Ib
25 Jan 55-1	123	3.02	.46	-.06	70	.23			s	6	1½	S	16	4.5	1.0	19.5	3.0	II
15 Feb 55-1	103	3.28	.39	-.13	70	.38			s	4	2	T	12	1.0	0.3	2.6	0.9	Ib
10 Mar 55-1	113	3.15	.42	-.12	70	.22			s	7	3	T						
22 Mar 55-1	110	3.18	.37	-.10	70	—								still water				D
6 Apr 55-1	109	3.20	.36	-.16	70	.53			s	3	2	T						
20 Apr 55-1	110	3.18	.38	-.05	70	.35			s	5	2	T						
29 Apr 55-1	134	2.90	.25	-.20	70	.29			s	5	2	T						

APPENDIX ID - Exposed Coast, D Range 70 ft and greater depths

1) Sampl. Date-Number	Median Diameter in Microns	2) Sediment Size Distribution Md_ϕ	σ_ϕ	α_ϕ	Depth of Water ft	Ripple Characteristics: Wave Length λ ft	Height η ft	Index $\frac{\lambda}{\eta}$	3) Symmetry $\frac{\beta}{\lambda}$	No. Meas.	4) Pattern	5) Profile	Waves: Period T sec	Orb. Diam. d_o ft	Orb. Veloc. u_m ft/sec	Hydraulic Condition $\frac{d_o}{\lambda}$	$\frac{u_m}{u_1}$	6) Type
5 May 55-1	124	3.01	.42	-.07	70	—								still	water			D
16 May 55-1	117	3.10	.40	-.05	70	.32			s	4	2	T						
8 Jun 55-1	112	3.16	.36	-.06	70	.30			s	6	2	T						
6 Jul 55-1	134	2.90	.32	-.06	70	.27			s	5	3	T	9	2.3	0.8	8.5	2.4	II
1 Aug 55-1	129	2.95	.42	-.02	70	.46			s	4	2	T						
10 Sep 55-1	113	3.15	.37	+.03	70	.44			s	4	3	T						
12 Oct 55-1	119	3.07	.39	-.10	70	.35			s	5	2	T						
23 Nov 55-1	125	3.00	.40	-.05	70	.34			s	5	1	T						
13 Jan 56-1	125	3.00	.45	-.04	70	.38			s	5	2	T						
30 Jan 56-1	122	3.03	.38	-.18	70	.27			s	6	1½	T						
10 Feb 54-1	103	3.28	.40	-.08	88	.32	.065	4.9	.63	5	1½	T						
11 Feb 54-1	81	3.63	.39	-.03	110	.33	.055	6.0	.49	5	2½	T	9	0.5	0.2	1.5	0.6	Ia
30 Mar 56	no sample				170	Ripples observed but not measured												

APPENDIX IIA - Exposed coasts, Pt. La Jolla and San Diego Area

2 Jul 54-2	556	.82	.28	-.07	8	1.88	.30	6.3	s	1	1	T	9	4.1	3.1	2.2	6.5	II
-2T	555	.85	.30	-.13														
2 Jul 54-1	484	1.05	.24	-.21	11	1.77	.30	6.0	s	2	1	T	9	2.5	2.4	1.4	5.5	Ic
-1T	486	1.04	.26	-.20														

APPENDIX IIA - Exposed coasts, Pt. La Jolla and San Diego Area (cont.)

1) Sample Date-Number	Median Diameter in Microns	2) Sediment Size Distribution Md_ϕ	σ_ϕ	α_ϕ	Depth of Water ft	Ripple Characteristics: Wave Length λ ft	Height η ft	Index $\frac{\lambda}{\eta}$	3) Symmetry $\frac{\beta}{\lambda}$	No. Meas.	4) Pattern	5) Profile	Waves: Period T sec	Orb. Diam. d_o ft	Orb. Veloc. u_m ft/sec	Hydraulic Condition $\frac{d_o}{\lambda}$	$\frac{u_m}{u_1}$	6) Type
4 Jul 56-1	637	.65	.21	-.05	19	2.80	0.5	5.6	s	1	1	T	15	9.0	2.2	3.2	4.3	II
-1T	633	.66	.23	-.13														
30 Nov 53-1	276	1.96	.50	-.22	30	1.20	.15	8.0	s	6	2½	T	9.7	4.1	1.3	3.4	3.7	II
-1T	257	1.96	.46	-.04														
15 Dec 53-2	325	1.62	.47	-.20	30	1.52	.22	6.9	.46	2	2	T	10.3	2.4	0.7	1.6	1.8	Ia
-2T	281	1.83	.49	-.02														
5 Jan 54-2	297	1.75	.48	-.19	30	.85			s	7	2	SW	10.0	2.9	0.9	3.4	2.5	II
-2T	254	1.98	.44	-.05														
14 Jan 54-2	457	1.13	.45	-.22	30	2.33	.37	6.3	s	4	1	S	10.0	2.8	0.8	1.2	1.9	Ia
-2T	379	1.40	.45	-.07														
2 Feb 54-3	415	1.27	.38	-.05	30	2.32	.35	6.7	.46	3	1	S	13	2.9	0.7	1.2	1.7	Ia
-3T	398	1.33	.39	-.13														
5 Feb 54-1	432	1.21	.42	-.12	30	2.25	.37	6.1	.44	1	1	S						
-1T	415	1.27	.39	-.03														
8 Feb 54-2	432	1.21	.34	-.06	30	2.67	.41	6.5	.49	1	1	S-T	12	3.5	0.9	1.3	2.1	Ia
-2T	392	1.35	.42	-.02														
9 Feb 54-1	441	1.18	.50	-.12	30	2.55	.44	5.8	.49	1	1	T	11	3.0	0.85	1.2	2.0	Ia
-1T	371	1.43	.46	-.02														
9 Feb 54-1	441	1.18	.50	-.12	30	2.64	.42	6.3	.42	1	1	T	11	3.0	0.85	1.1	2.0	Ia
-1T	371	1.43	.46	-.02														
9 Aug 54-1	514	0.96	.35	+.01	30	2.65	.45	5.9	o	1	1	S	12	2.6	0.7	1.0	1.5	Ia
-T	418	1.26	.40	-.02														
9 Aug 54-2	222	2.17	.92	0	40	.80				2	2	T	12	3.1	0.8	3.9	2.3	II

APPENDIX IIA - Exposed coasts, Pt. La Jolla and San Diego Area (cont.)

1) Sample Date-Number	Median Diameter in Microns	2) Sediment Size Distribution Md_ϕ	σ_ϕ	α_ϕ	Depth of Water ft	Ripple Characteristics: Wave Length λ ft	Height η ft	Index $\frac{\lambda}{\eta}$	3) Symmetry $\frac{\beta}{\lambda}$	No. Meas.	4) Pattern	5) Profile	Waves: Period T sec	Orb. Diam. d_o ft	Orb. Veloc. u_m ft/sec	Hydraulic Condition: $\frac{d_o}{\lambda}$	$\frac{u_m}{u_1}$	6) Type
10 Aug 54-1	419	1.28	.34	+.03	40	2.80				1	1	T			short per. complex			
-1T	212	2.24	.45	-.07														
10 Aug 54-2A	321	1.64	.54	-.14	40	2.00				1	1	T						
-2AT	261	1.94	.72	0														
10 Aug 54-2B	274	1.87	.56	-.05	40	.90						T						
-2BT	247	2.02	.69	+.15														
10 Aug 54-3	129	2.95	.64	-.33	40	.47				6	2	T						
-3T	122	3.04	.65	-.30														
10 Aug 54-6	164	2.61	.98	-.80	40	.51				4	2½	T						
18 Aug 54																		
-1(0-1cm)	398	1.33	.62	+.05	40	2.05	.31	6.6	s	1	1	T	8	2.5	1.0	1.2	2.5	Ic
-1(5-6cm)	287	1.80	1.01	+.40									short period superimposed					
-1T	342	1.55	.95	+.40														
1 Oct 54-1	551	0.86	.51	+.05	40	2.14	.36	5.9	.36	1	1	T						
-1T	293	1.77	1.10	+.30														
1 Aug 56-1	359	1.48	.30	+.12	45	2.60	.40	6.5	o	1	1	T	11	3.1	0.8	1.2	2.0	Ia
-1T	330	1.60	.42	+.19														
30 Nov 53-2	470	1.09	.37	-.14	55	3.00	.48	6.2	s	1	2	T	9.7	2.9	0.9	1.0	2.0	Ia
-2T	426	1.23	.52	+.17														
15 Dec 53-1	525	.93	.34	-.03	55	3.00	.48	6.2	.54	4	1	S	10.3	2.2	0.6	0.7	1.3	Ia
-1T	399	1.33	.64	+.17														
16 Dec 53-1	501	.99	.28	+.04	55	2.89	.52	5.6	.48	4	1	S						
29 Jan 54-1	432	1.21	.36	+.03	55	2.53	.39	6.5	s	2	1	S&T	11	2.3	.65	0.9	1.5	Ia
-1T	415	1.27	.64	+.02														

APPENDIX IIA - Exposed Coasts , Pt. La Jolla and San Diego Area (cont.)

1) Sample Date-Number	Median Diameter in Microns	2) Sediment Size Distribution Md_ϕ	σ_ϕ	α_ϕ	Depth of Water ft	Ripple Characteristics: Wave Length λ ft	Height η ft	Index $\frac{\lambda}{\eta}$	3) Symmetry $\frac{\beta}{\lambda}$	No. Meas.	4) Pattern	5) Profile	Waves: Period T sec	Orb. Diam. d_o ft	Orb. Veloc. u_m ft/sec	Hydraulic Condition: $\frac{d_o}{\lambda}$	$\frac{u_m}{u_1}$	6) Type
8 Feb 54-1	448	1.16	.36	+.11	55	2.72	.44	6.2	.66	1	1	S-T	12	3.2	0.8	1.2	1.9	Ia
-1T	412	1.28	.52	-.04														
28 Jul 54-1	124	3.01	.50	-.34	85	.49	0.10	4.9	s	10	2	T						
-1T	124	3.01	.49	-.35														
3 Aug 54-1	165	2.60	.62	-.25	85	.68	.13	5.2	s	2	2	T						
-1T	127	2.98	.56	-.30														
3 Aug 54-2	335	1.59	.59	-.15	85	2.70			s	1	2	T						
-2T	342	1.55	.65	+.15														
31 Mar 54-1	88	3.50	.44	-.25	110	.34			s	5	2	T						
14 Jan 55-3	132	2.92	.50	-.12	120	.47			s	3	2	S						

APPENDIX IIB - Exposed Coast, Point Dume, Calif.

8 Sep 54-18	913	0.13	1.02	+.36	7	3.45	.65	5.3	o	1	1	T	13	3.5	1.3	1.0	2.1	Ic
-18T	319	1.65	1.15	-.42														
8 Sep 54-14	254	1.98	.70	-.30	11	.59			s	2	2	T	13	2.0	1.2	3.4	3.4	II
9 Sep 54-27	120	3.06	.31	-.15	38	.34				3	2	T	8	.9	.35	2.6	1.0	Ib
8 Sep 54-10	149	2.73	.60	-.14	47	.48			s	2	2½	T	13	1.5	.4	3.1	1.2	Ib

APPENDIX IIC - Exposed Coast, Guadalupe Island, Mexico

15 Nov 54-6	122	3.04	.41	-.17	61	.25				6	1	T						

APPENDIX IIC - Exposed Coast, Quadalupe Island, Mexico (cont.)

1) Sample Date-Number	Median Diameter in Microns	2) Sediment Size Distribution $M_{d\phi}$	σ_ϕ	α_ϕ	Depth of Water Ft	Ripple Characteristics: Wave Length λ ft	Height η ft	Index $\frac{\lambda}{\eta}$	3) Symmetry $\frac{\beta}{\lambda}$	No. Meas.	4) Pattern	5) Profile	Waves: Period T sec	Orb. Diam. d_o ft	Orb. Veloc. u_m ft/sec	Hydraulic Condition $\frac{d_o}{\lambda}$	$\frac{u_m}{u_1}$	6) Type
15 Nov 54-7	460	1.12	.84	-.14	61	4.00	.75	5.3	s	1	1	T						
15 Nov 54-8	379	1.40	.66	-.15	66	2.20			s	1	1	T				•		

APPENDIX IID - Surge Channel off Pt. Loma, San Diego, Calif. (special case).

14 Jan 55-1	2603	-1.38	.70	-.04	45	4.10												
-1T	3317	-1.73	1.22	-.13														

APPENDIX IIIA - Protected Coast, Santa Catalina Harbor

10 Sep 54-5	460	1.12	.68	+.15	4½	1.80	.30	6.0	s	1	1	S	10	2.2	1.2	1.2	2.7	Ic
-5T	1395	-0.48	1.97	-.45														
10 Sep 54-6	457	1.13	.80	-.45	4½	1.75	.25	7.0	s	1	1	S	10	2.2	1.2	1.3	2.7	Ic

APPENDIX IIIB - Protected Coast, Wilson Cove, San Clemente Island.

12 Jun 56-4	173	2.53	.58	-.02	21	.67	.10	6.7	s	1	1	T		sheltered lee				
-4T	162	2.63	.58	-.12														

APPENDIX IIIC - Protected Coast, Los Coronados Islands, Mexico

9 Feb 56-1	245	2.03	.39	-.18	35	.75			s	2	2	T		sheltered lee				
-1T	242	2.05	.40	-.17														
13 Jan 55-1	113	3.15	.38	-.05	65	.20				1	3	T		sheltered lee				
13 Jan 55-2	555	.85	.54	-.57	65	1.10	.25	4.4	s	1	2	T		sheltered lee				

APPENDIX IVA - Limited Fetch, Mission Bay, California

1) Sample Date-Number	Median Diameter in Microns	2) Sediment Size Distribution Md_ϕ	σ_ϕ	α_ϕ	Depth of Water ft	Ripple Characteristics: Wave Length λ ft	Height η ft	Index $\frac{\lambda}{\eta}$	3) Symmetry $\frac{\beta}{\lambda}$	No. Meas.	4) Pattern	5) Profile	Waves: Period T sec	Orb. Diam. d_o ft	Orb. Veloc. u_m ft/sec	Hydraulic Condition $\frac{d_o}{\lambda}$	$\frac{u_m}{u_1}$	6) Type
20 Jan 55-1	195	2.36	.49	-.14	0.16	.14	.020	7.0	s	5	1	T	0.7	0.15	0.4	1.1	1.2	Ia
-1T	237	2.08	.53	-.06														
20 Jan 55-2	123	3.02	.45	-.13	0.16	.15	.025	6.0	s	4	1	T	0.7	0.15	0.4	1.0	1.2	Ia
20 Jan 55-3	233	2.10	.45	+.04	0.11	.14			o	4	1	T	.45	.13	0.4	0.9	1.2	Ia

APPENDIX IVB - Hawaiian Islands (Lagoon Inside Reef)

8 Dec 55-62	344	1.54	.62	-.40	4.0	2.30	.38	6.1	o	1	1	T	3½	2.8	1.3	1.2	3.4	Ic
-62T	295	1.76	.60	-.50														
13 Dec 55-2	595	.75	.94	-.16	7	1.05	.16	6.5	s	1	1	T	3½	1.3	1.2	1.2	2.4	Ic

APPENDIX IVC - Beach Erosion Board, Model Wave Tank

	221	2.18			.40	.33	.055	6.0	.35	1		T	2.12	.38	.7	1.2	2.1	Ia

APPENDIX V

COMPUTATION OF ORBITAL VELOCITIES AND DISPLACEMENTS NEAR THE BOTTOM

There appears to be no single wave theory which is both capable of reliable prediction of the various wave properties from deep water into the surf zone, and which is in a practical form for their computation. For this reason it seemed expedient to use different techniques for computing orbital velocities and displacements near the surf zone from those used in deeper water. In general, the Airy theory for waves of small amplitude was used in deeper water, and an adaptation of solitary wave theory was used when waves were near the breaker zone. The two techniques are described below together with a criterion for their use.

AIRY WAVES

The classical theory of wave motion, attributed to Airy in 1845, is strictly applicable to waves of infinitely small height in water of any depth. The wave profile is sinusoidal and the particle orbits are closed circles in deep water and ellipses in shallow water. The orbital velocities and particle displacements vary as sine functions with time, and their maximum magnitudes in onshore and offshore directions are equal.

The instantaneous horizontal displacement, r, of a water particle from its equilibrium position for an Airy wave is:

$$r = -\frac{H}{2}\frac{\cosh 2\pi \frac{z}{L}}{\sinh 2\pi \frac{h}{L}} \sin \frac{2\pi}{L}(x - Ct) \qquad (1)$$

where $L = CT$ is the wave length, h is the depth of water, C, T, and H, are the wave phase velocity, period, and height respectively, z is the vertical coordinate measured from the bottom upwards, and x and t are the horizontal distance and time measured from the wave crest. The total range of horizontal displacement, or orbital diameter d, is equal to twice the absolute maximum value of r. Near the bottom this reduces to

$$d_o = \frac{H}{\sinh 2\pi \frac{h}{L}} \qquad (2)$$

The maximum horizontal component of orbital velocity occurs at the instant of wave crest and trough passage, and near the bottom is given by

$$u_m = \frac{\pi d_o}{T} \qquad (3)$$

The computation of d_o and u_m is facilitated by tables of $\sinh 2\pi \frac{h}{L}$ as function of the depth and deepwater wave length (Beach Erosion Board Technical Report No. 4).

SOLITARY WAVE

In shallow water and near the breaker zone the continuous frequency characteristics commonly associated with waves in deep water are lost and individual waves tend to retain their identity and in many ways resemble the solitary wave of Scott-Russell. For this reason the solitary wave concept has been applied to waves near the breaker zone and has met with some degree of success. Munk (1949) summarized useful relations derived from solitary wave theory and made them accessible to numerical example and Inman and Nasu (1956) compared measurements of orbital velocity of ocean waves with theory. The later study suggests that a reasonable proximation to the horizontal orbital velocities of water particles near the bottom can be obtained from solitary theory.

According to solitary theory, water particles are essentially at rest at some distance in front of the wave crest. As the crest approaches they move forward and upward and attain their maximum velocity at the instant of crest passage. Following the passage of the crest the velocity of the particles decreases and they move downward, eventually reaching a new rest position a distance 2r in advance of their former rest position. Thus, when solitary waves travel through still water, particles undergo relatively flat trajectories with motion only in the direction of wave propagation. Closed or partially closed trajectories and orbital motion more nearly resembling that of shallow water waves in nature are obtained from the theory by superposing some sort of return flow on the solitary wave.

The condition of no return flow, or of solitary waves traveling through still water, leads to a maximum net particle displacement at the bottom with the passage of each wave crest. The net displacement decreases and the trajectory becomes more orbital in nature as the return flow increases. The net displacement becomes zero when the return flow, $\bar{v}$, is equal to the still water displacement, 2r, divided by the wave period. Although the condition of zero net particle displacement along the bottom is certainly not rigorously fulfilled in nature, on the whole such an assumption may give a reasonable approximation to conditions generally encountered in shallow water. However, applications of concepts of this type to conditions in nature are at best only approximate; and are subject among other things, to the limitation imposed by Bagnold (1947) and Munk (1949). An important limiting criterion, that the period of the waves must be equal to or greater than the effective period, is discussed later.

The particle displacement due to a solitary wave traveling through still water, and the orbital diameter of the particle trajectory for the special case in which there is no net particle displacement at the bottom are derived below, and graphs for their computation are given in Plates 1 and 2.

Solitary Wave in Still Water

Following approximately the dimensionless notation of Munk (1949, eq. 31), the McCowan equation for the horizontal component of orbital velocity along the bottom is

$$U = \frac{N}{1 + \cosh M X} \tag{4}$$

where $u = CU$ is the horizontal component of orbital velocity, $x = hX$ is the horizontal distance measured from the wave crest, $C = \sqrt{g(h+H)}$ is the velocity of propagation of the wave crest, H is the wave height, h is the depth of water under the wave trough, M and N are functions of the relative wave height, $\gamma = H/h$, and are defined by the equations

$$\gamma = \frac{N}{M} \tan 1/2 \left[M(1 + \gamma)\right] \tag{5}$$

$$N = 2/3 \sin^2 \left[M(1 + 2/3\ \gamma)\right] \tag{6}$$

If r is the horizontal displacement of a water particle at time t relative to its position at the instant of passage of the wave crest, then (Munk, 1949, eq. 14)

$$r = \int_0^t u\,dt = \int_0^x \frac{u}{C-u}\,dx \tag{7}$$

where $dx = (C-u)\,dt$. In dimensionless notation

$$R = \frac{r}{h} = \int_0^X \frac{U}{1 - U}\,dX \tag{8}$$

Substituting the value of U from equation (4) and taking twice the value of the integral to include the displacement preceding the passage of the wave crest

$$2R = 2\frac{N}{M}\int_0^X \frac{dMX}{(1-N) + \cosh MX} = \left[4\frac{N}{M}\,k \csc \beta\right]_0^X \tag{9}$$

where $\cos \beta = 1 - N$: $\tan k = \left[\tanh \frac{MX}{2}\right]\left[\tan \frac{\beta}{2}\right]$

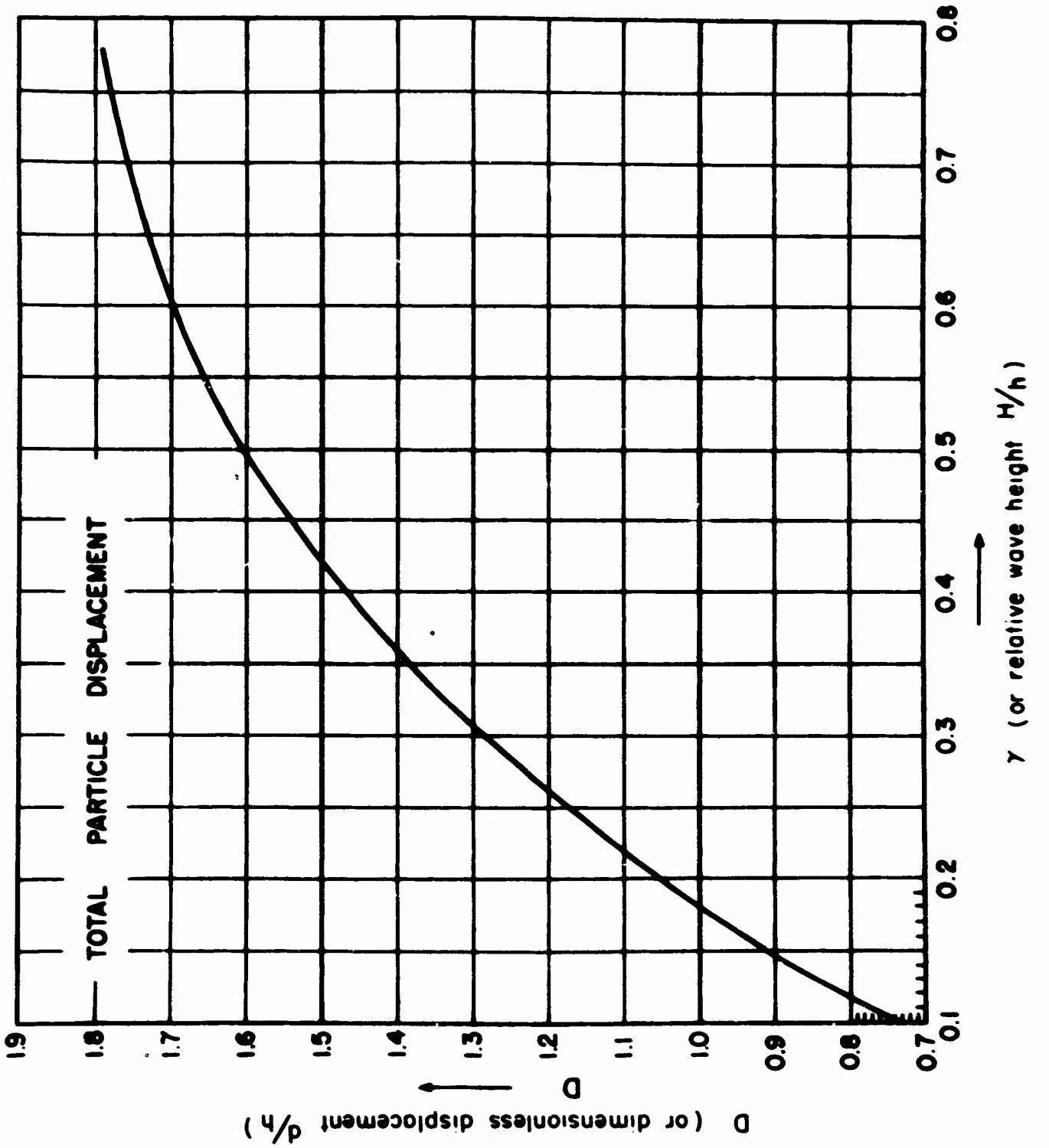

PLATE V-1. TOTAL PARTICLE DISPLACEMENT AT THE BOTTOM FOR A SOLITARY WAVE TRAVELING THROUGH STILL WATER, (EQUATION 10).

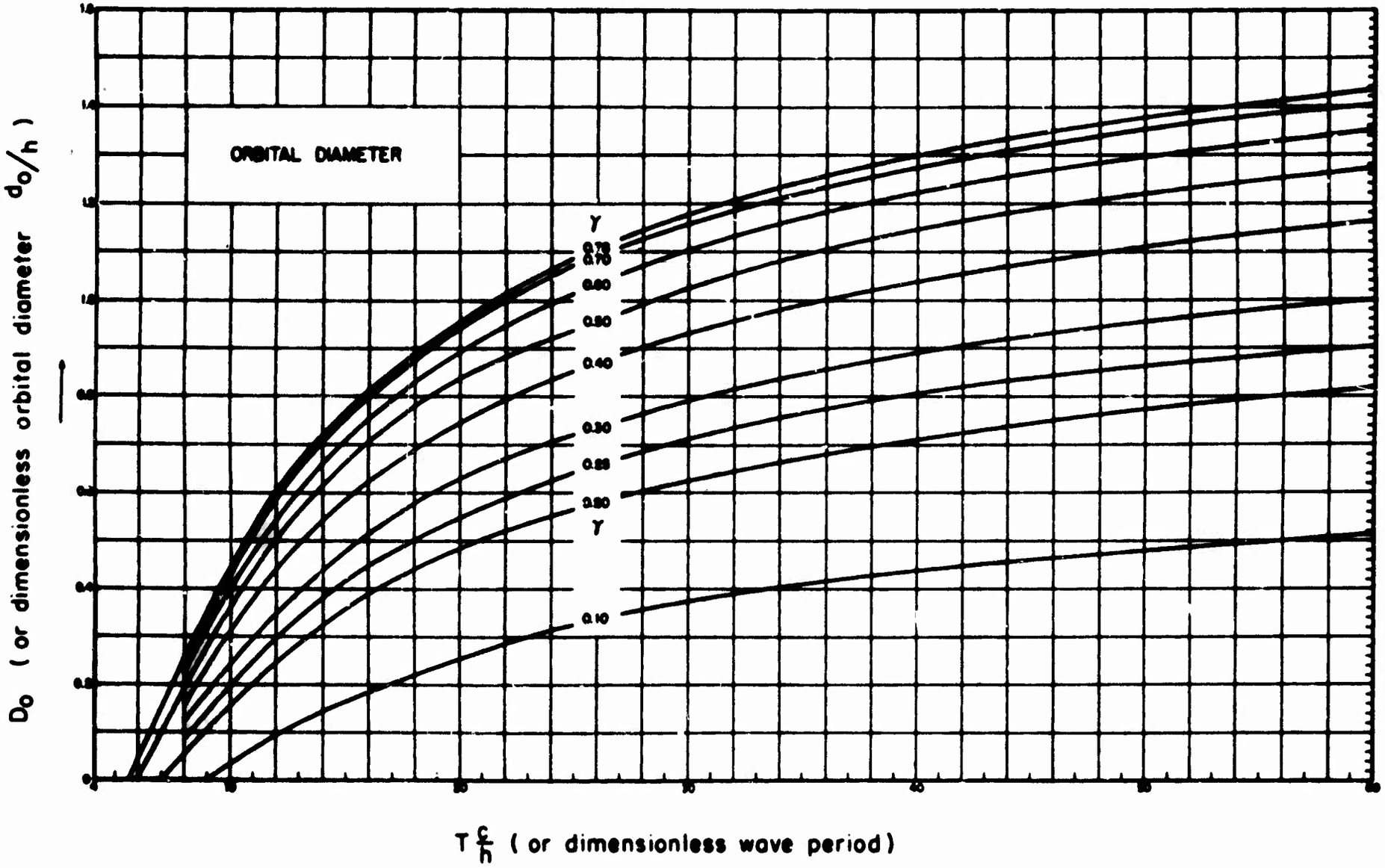

PLATE V-2. HORIZONTAL ORBITAL DIAMETER FOR THE CLOSED ORBIT TRAJECTORY OF A SOLITARY WAVE, (EQUATION 15).

For the case where X is taken to infinity, the total particle displacement is given by

$$D = 2R = \frac{2N}{M} \beta \csc \beta \qquad (10)$$

The dimensionless displacement D is graphed as a function of the relative wave height γ in Plate 1. To convert the displacement to conventional units it is necessary to multiply D by the depth of water, $d = hD$.

Closed Orbit Displacement

If it is assumed that there is no net displacement of a water particle along the bottom due to solitary wave motion, then a dimensionless return flow $\bar{V}$, opposed in direction to that of the wave propagation, is defined

$$\bar{V} = \frac{D}{T \frac{C}{h}} \qquad (11)$$

where D is given by equation (10), T is the wave period, and $T \frac{C}{h}$ is the dimensionless wave period.

Under these conditions, and relative to a coordinate system moving with the wave crest, a water particle will move forward during the passage of a solitary wave crest a distance X_1 until the orbital velocity U decreases to the value of $\bar{V}$, at which time the particle will reach a maximum forward position in its trajectory. It will then move backward under the influence of the return flow, past its initial position to a position $-X_1$. The following wave crest will then cause the particle to move forward again when the orbital velocity exceeds the return flow, and the trajectory for the closed orbit will be completed. X is obtained from equation (4) by setting U equal to the return velocity V.

Relative to the moving coordinate system, the total displacement imparted to a water particle during the propagation of the wave crest from $-X_1$ to $+X_1$ is given by 2R, in equation (9). It remains to evaluate the transit time, $2t_1$ of the particle between $-X_1$ and $+X_1$.

Since the wave crest is advancing with phase velocity C, relative to a fixed point on the bottom, the water particle will have advanced a distance r_1 and the wave crest will advance a distance $r_1 + x_1$ during time t_1. Thus in moving from -x to +x the water particle is acted on by the return flow $\bar{V}$ for a time.

$$2t_1 = \frac{2(r_1 + x_1)}{C} \qquad (12)$$

or in dimensionless notation

$$2t_1 \frac{C}{h} = 2 (R_1 + X_1) \tag{13}$$

In time $2t_1$ the water particle is moved backwards by the return flow $\bar{V}$ a total distance

$$2R_2 = 2 \bar{V} (R_1 + X_1) \tag{14}$$

and during the same time the particle is carried forward by the orbital motion of the solitary wave a distance $2R_1$. Therefore, the total horizontal orbital diameter of the closed orbit trajectory becomes

$$D_o = 2(R_1 - R_2) \tag{15}$$

The dimensionless orbital diameter D_o is graphed as a function of relative wave height γ and dimensionless wave period $T \frac{C}{h}$ in Plate 2. To convert the orbital diameter to conventional units it is necessary to multiply by the water depth h,

$$d_o = h D_o \tag{16}$$

Closed Orbit Velocities

Under the assumption that the wave motion is solitary in nature and that the trajectories of water particles form closed orbits along the bottom, the maximum horizontal orbital velocities under wave crests and troughs can be computed from the above relations. If the wave length is very great compared to the depth of the water, the maximum backward velocity under the wave trough is simply equal to the net return flow defined in equation (11), which when converted to conventional notation is

$$u_t = \frac{hD}{T} \tag{17}$$

Referring to equation (4), directly beneath the wave crest X is zero and the horizontal velocity along the bottom becomes, in conventional notation,

$$u = \frac{1}{2} NC \tag{18}$$

This is the maximum horizontal velocity along the bottom for a solitary wave traveling through still water. The maximum horizontal velocity under the wave crest for the special case of a closed orbit trajectory then becomes

$$u_c = u - u_t \tag{19}$$

Values of u for various water depths and wave heights are graphed in Inman and Nasu (1956, Figure 27).

Field measurements of orbital velocity made just seaward of the breaker zone by Inman and Nasu (1956, table 2b) showed the ratio of the maximum crest to maximum trough velocity to range from about 1 to 4. If for practical purposes it is assumed that the ratio does not exceed 4, then as an upper limit the maximum crest velocity will not exceed 80% of the maximum still water velocity given by equation 18. Thus in regions where the solitary theory applies, the maximum horizontal orbital velocity under the wave crest, u_m, is arbitarily defined as being equal to u_c, but not to exceed $0.8^m u$.

$$u_m = u_c \leq 0.8\, u \tag{20}$$

Effective Wave Length and Period

Application of solitary theory to orbital velocities and displacements requires, among other things, that the wave crests be sufficiently far apart to permit the assumption that a water particle comes to rest following the passage of each wave crest when the solitary model is traveling in still water. An effective wave length $L_e = 2X$ can be defined where X is the distance from the wave crest necessary to reduce the orbital velocity to some acceptable fraction, f, of the maximum velocity under the wave crest. From equations (4) and (18) the dimensionless distance from the crest becomes

$$X = \frac{\cosh^{-1}\left(\frac{2}{f} - 1\right)}{M} \tag{21}$$

from which an effective wave period is obtained

$$T_e = \frac{2\,X\,h}{C} \tag{22}$$

If we assume that a reduction in orbital velocity to 2-1/2 percent of the maximum crest velocity is sufficient to permit application of solitary theory, then f = 1/40, and X equals approximately $\frac{5}{M}$, from which the effective period becomes

$$T_e = \frac{10}{M}\,\frac{h}{C}$$

This is not necessarily a conservative estimate for T_e because the reduction in wave velocity by the return flow is not considered in computing C. Therefore it was assumed that the solitary theory could

apply only when the dimensionless wave period was somewhat greater than $\frac{10}{M}$,

$$T \frac{C}{h} > \frac{10}{M} \qquad (23)$$

This requirement is somewhat more conservative than the effective period defined by Bagnold (1947) and used by Munk (1949), $T_e = \frac{2\pi}{M}\sqrt{\frac{h}{g}}$.

SAMPLE COMPUTATION

Given

H, wave height ..... 4 ft

h, water depth under wave trough . 8 ft

T, wave period ..... 10 sec

Computation

γ , relative wave height H/h 0.5

M , and N (from Munk 1949, plate 5) ..... 0.88 & 0.57

C , wave velocity $\sqrt{g\ (h + H)}$ ..... 19.6 ft/sec

Dimensionless wave period $T \frac{C}{h} > \frac{10}{M}$ ..... 24.5 > 11.4

∴ Solitary theory applies

* * * * * * * * * * *

D , dimensionless particle displacement (still water) plate 1.... 1.6

D_o, dimensionless orbital diameter (closed orbit) plate 2..... 0.93

d_o, orbital diameter (closed orbit), hD_o ..... 7.4 ft

u , maximum orbital velocity (still water), equation 18, or Inman and Nasu, 1956, figure 27 ..... 5.6 ft/sec

u_t, max. orbital velocity under trough (closed orbit), eq. 17 ... 1.3 ft/sec

u_c, max. orbital velocity under crest (closed orbit), $u - u_t$ .... 4.3 ft/sec

u_m, practical max. orbital velocity equals $u_c < 0.8\ u$, equation 20 ..... 4.3 ft/sec